Coexisting Attractors and Complex Basins in Discrete-time Economic Models

Gian Italo Bischi [†] and Fabio Lamantia [‡]

[†] Istituto di Scienze Economiche, University of Urbino, Urbino, Italy
[‡] S.A. Department, University of Calabria, Arcavacata di Rende (CS), Italy

Abstract In this lesson we consider discrete time dynamical systems with coexisting attractors, and we analyze the problem of the structure of the boundaries that separate their basins of attraction. This problem may become particularly challenging when the discrete dynamical system is represented by the iteration of a noninvertible map, because in this case nonconnected basins can be obtained, formed by several (even infinitely many) disjoint portions. Measure theoretic attractors, known as Milnor attractors, are also described, together with riddled basins, an extreme form of complex basin's structure that can be observed in the presence of such attractors. Some tools for the study of global bifurcations that lead to the creation of complex structures of the basins are described, as well as some applications in discrete time models taken from economic dynamics.

1 Introduction

Many mathematical models of social, economic and financial systems are characterized by the interaction among boundedly rational agents, that try to obtain their goals by adaptive processes, based on "trial and error" or "learning by doing" methods. This implies that the mathematical modelling of these processes, where decisions are repeatedly taken over time, are formulated as deterministic discrete time dynamical systems, i.e. their time evolution is expressed by the repeated application (iteration) of a map $T : S \to S$, where $S \subseteq \mathbb{R}^n$. If the state of the economic system is described by a vector $x \in S$, starting from an initial condition $x_0 \in S$ the time evolution of the system is expressed by a sequence of states $x(t)$, $t \in \mathbb{N}$, obtained *inductively* by the iteration of a map defined by $x' = T(x)$, where the right hand side represents the state at the time period t, and the left hand side represents the state at the time $(t+1)$.

It is worth to notice that discrete time dynamical systems are sometimes obtained through some discretization procedure applied to continuous time models, as often happens in physics or biology. Instead, economic time is often intrinsically discrete, because decisions in economics cannot be continuously revised. As trivial example to illustrate this point, let us consider a farmer that decides how much wheat has to be sowed: such a decision cannot be revised until next sowing season.

The dynamic models in economics are generally nonlinear, and it is now well known that even one-dimensional discrete nonlinear dynamical systems may exhibit complex asymptotic behaviors, due to the existence of chaotic attractors.

Moreover, nonlinearity may also imply that several equilibria may coexist. For example, dynamic games often have several equilibria (see, among others, Binmore, 1992, Weibull, 1995) and in many models with expectations and learning several rational expectations equilibria are present, or rational equilibria coexist with non rational ones (Guesnerie and Woodford, 1993). In these cases, an adaptive process may become an equilibrium selection device, as it allows one to distinguish between stable and unstable equilibria. However, in many models with evolutive (or learning) mechanism, a situation denoted as "multistability" is present, i.e. several attractors exist, each with its own basin of attraction. Consequently, selection criteria based on local stability are not sufficient to identify the long run evolution of the system, and the dynamic process becomes path-dependent: the long run dynamics depend on the starting condition, and a thorough knowledge of the basins and their structure becomes crucial for the researcher to be able to predict which one of the multiple equilibria is more likely to be observed (see e.g. Lorenz, 1992, Soliman, 1999, Barucci et al., 1999, Bischi and Kopel, 2001, Bischi et al., 2003a,b, Agliari et al., 2002, Bischi et al., 2004).

This leads to the question of the delimitation of the basins of attraction and their changes as the parameters of the model vary. This issue cannot be studied by local methods (i.e. based on linear approximations around the attractors) but through a global study of the map, often requiring an interplay among analytical, geometric and numerical methods (see e.g. Brock and Hommes, 1997, Bischi et al., 2000a, Puu, 2000, Agliari et al., 2002). The existence of complex topological structure of the basins becomes particularly intriguing when dealing with discrete dynamical systems represented by the iteration of noninvertible maps (see Mira et al., 1996, Abraham et al., 1997, and references therein). Moreover the complexity related to the structure of the basins is not related, in general, to the existence of chaotic attracting sets, in the sense that simple attractors (e.g. stable steady states) may have basins with a complicated topological structure whereas complex attractors, e.g. strange attractors, may exist whose basins have simple boundaries.

In the last two decades, the literature on economic dynamics has mainly been devoted to the study of the attractors and their qualitative changes (bifurcations) leading to more and more complex kinds of asymptotic dynamics (fixed points, cycles, quasi-periodic orbits, chaotic attractors). Such routes to more and more complex behaviors, as some parameters are varied, have been characterized by sequences of local bifurcations (such as the well known period doubling route to chaos) and by global bifurcations, typically homoclinic bifurcations. Instead, the complexity related to the structure of basins leads to a different kind of sensitivity with respect to slight changes of initial conditions. In fact, if a point is far from the basin boundaries, a slight perturbation has no effect on the long run behavior, whereas if a point is very close to a basin boundary (and many point are in such a situation in the presence of complex basin boundaries) a small perturbation has a high probability to cause a crossing of the boundary and consequently the long run evolution will be very different, i.e. the trajectory may go to a completely different region of the phase space (it may even diverge). This kind of sensitivity is different from the sensitive dependence on initial conditions which characterizes a chaotic attractor. In fact, in this case, even if two initially very close chaotic trajectories quickly depart as time increases (at an exponential rate), such trajectories are finally trapped inside the same compact invariant set (the chaotic attractor).

Both the questions outlined above require an analysis of the global dynamical properties of the dynamical system, that is, an analysis which is not based on the linear approximation of the map. When the map is noninvertible the global dynamical properties can be usefully characterized by the method of critical sets, a powerful tool introduced in the seventies (see Gumovski and Mira, 1980, Mira et al. 1996, Abraham et al. 1997) but only recently employed in the study of dynamic modelling of economic and financial systems (see e.g. Bischi et al., 1999a, Kopel et al., 2000, Puu 2000, Bischi and Kopel, 2001, Bischi et al., 2003a,b, Dieci et al., 2001, Chiarella et al., 2001, 2002). Indeed, several discrete time models of economic systems are represented by the iteration of a noninvertible map, i.e. a point transformation T which maps distinct points into the same point. Loosely speaking, this can be expressed by saying that the map "folds and pleats" the state space. As we shall describe in the following, the folding action associated with the application of a noninvertible map, as well as the "unfolding" associated with the geometric action of the inverses, can be described by using the formalism of critical sets. The repeated application of a noninvertible map repeatedly folds the state space along the critical sets and their images, and often this allows one to define a bounded region where asymptotic dynamics are trapped. Instead, the repeated application of the inverses "repeatedly unfolds" the state space, so that a neighborhood of an attractor may have preimages far from it. This may give rise to complicated topological structures of the basins, whose detection can be explained on the basis of the global properties of the dynamical system, as explained below.

The lesson is organized as follows. In section 2 we recall some definitions and properties concerning discrete dynamical systems represented by noninvertible maps. In section 3 we consider the problem of the delimitation of the basins in one-dimensional discrete dynamical systems, and we give some examples of global bifurcations that cause the creation of nonconnected basins. In section 4 we consider two-dimensional discrete dynamical systems, recalling some recent examples of two-dimensional dynamic models taken from the economic literature. In section 5 we consider the case of dynamical systems that have invariant submanifolds of lower dimension with respect to the state space, where chaotic Milnor attractors are embedded, and we analyze the related phenomena of chaos synchronization and riddled basins. We also show how such particular dynamic situations arise in competition models.

2 Some basic definitions and properties

In this section we give some basic definitions and properties, and a minimal vocabulary, about discrete dynamical systems, with a particular emphasis on the ones represented by the iteration of noninvertible maps. A map $T : S \to S$, $S \subseteq \mathbb{R}^n$, defined by $x' = T(x)$, transforms a point $x \in S$ into a unique point $x' \in S$. The point x' is called the *rank-1 image* of x, and a point x such that $T(x) = x'$ is a *rank-1 preimage* of x'. A *discrete-time dynamical system* is defined inductively by the difference equation

$$x(t+1) = T(x(t)) \tag{2.1}$$

where x represents the state of a system, and T can be seen as a "unit time advancement operator" $T : x(t) \to x(t+1)$. Starting from an *initial condition* $x_0 \in S$, the repeated

application (*iteration*) of T uniquely defines a *trajectory*

$$\tau(x_0) = \left\{x(t) = T^t(x_0), t = 0, 1, 2, ...\right\}, \tag{2.2}$$

where T^0 is the identity map and $T^t = T(T^{t-1})$.

A set $A \subset \mathbb{R}^n$ is *trapping* if it is mapped into itself, $T(A) \subseteq A$, i.e. if $x \in A$ then $T(x) \in A$. A trapping set is *invariant* if it is mapped onto itself: $T(A) = A$, i.e. all the points of A are images of points of A.

A closed invariant set A is an *attractor* if it is *asymptotically stable,* that is

(i) it is *Lyapunov stable,* i.e. for every neighborhood W of A there exists a neighborhood V of A such that $T^t(V) \subset W \ \forall t \geq 0$

(ii) a neighborhood U of A exists such that $T^t(x) \to A$ as $t \to +\infty$ for each $x \in U$.

The *basin* of an attractor A is the set of all points that generate trajectories converging to A

$$\mathcal{B}(A) = \left\{x \mid T^t(x) \to A \quad \text{as} \quad t \to +\infty \right\} \tag{2.3}$$

Let $U(A)$ be a neighborhood of an attractor A whose points converge to A. Of course $U(A) \subseteq \mathcal{B}(A)$, and also the points that are mapped into U after a finite number of iterations belong to $\mathcal{B}(A)$. Hence, the basin of A is given by

$$\mathcal{B}(A) = \bigcup_{n=0}^{\infty} T^{-n}(U(A)) \tag{2.4}$$

where $T^{-1}(x)$ represents the set of the *rank-1* preimages of $\mathbf{x}$ (i.e. the points mapped into x by T), and $T^{-n}(x)$ represents the set of the *rank-n* preimages of x (i.e. the points mapped into x after n applications of T).

Let $\mathcal{B}$ be a basin of attraction and $\partial\mathcal{B}$ its boundary. From the definition it follows that $\mathcal{B}$ is trapping with respect to the forward iteration of the map T and invariant with respect to the backward iteration of all the inverses T^{-1}, that is, $T(\mathcal{B}) \subseteq \mathcal{B}$ and $T^{-1}(\mathcal{B}) = \mathcal{B}$. The same relations hold for the points located along the boundary, i.e.

$$T(\partial\mathcal{B}) \subseteq \partial\mathcal{B}, T^{-1}(\partial\mathcal{B}) = \partial\mathcal{B}. \tag{2.5}$$

This implies that if an unstable fixed point or cycle belongs to $\partial\mathcal{B}$ then $\partial\mathcal{B}$ must also contain all its preimages of any rank. Moreover, if a saddle-point, or a saddle-cycle, belongs to $\partial\mathcal{B}$, then $\partial\mathcal{B}$ must also contain the whole stable set (see Gumowski and Mira 1980, Mira et al. 1996).

From (2.4) and (2.5) follows that in order to study the extension of a basin and structure of its boundaries one has to consider the backward iteration of T. So, the invertibility of T and the properties of the inverse relation T^{-1} must be considered. We recall that if $x \neq y$ implies $T(x) \neq T(y)$ for each x, y in S, then T is an *invertible map* in S, because the inverse mapping that gives $x = T^{-1}(x')$ is uniquely defined; otherwise T is said to be a *noninvertible map*, because points x exist that have several *rank-1* preimages, i.e. the inverse relation $x = T^{-1}(x')$ may be multivalued. So, noninvertible means "many-to-one", that is, distinct points $x \neq y$ may have the same image, $T(x) = T(y) = x'$. Geometrically, the action of a noninvertible map T can be expressed by saying

that it "folds and pleats" the space S, so that the two distinct points are mapped into the same point. This is equivalently stated by saying that several inverses are defined in some points of S, and these inverses "unfold" S.

For a noninvertible map S can be subdivided into regions Z_k, $k \geq 0$, whose points have k distinct *rank-1* preimages. Generally, as the point x' varies in $\mathbb{R}^n$, pairs of preimages appear or disappear as this point crosses the boundaries separating different regions. Hence, such boundaries are characterized by the presence of at least two coincident (merging) preimages. This leads to the definition of the critical sets, one of the distinguishing features of noninvertible maps (Gumowski and Mira, 1980, Mira et al., 1996):

Definition. The *critical set* CS of a continuous map T is defined as the locus of points having at least two coincident *rank-1* preimages, located on a set CS_{-1} called *set of merging preimages*.

The critical set CS is generally formed by $(n-1)$-dimensional hypersurfaces of $\mathbb{R}^n$, and portions of CS separate regions Z_k of the phase space characterized by a different number of *rank-1* preimages, for example Z_k and Z_{k+2} (this is the standard occurrence). As we shall see below, the critical set CS is the n-dimensional generalization of the notion of local minimum/maximum value of a one-dimensional map, and of the notion of *critical curve* LC of a noninvertible two-dimensional map[1]. The set CS_{-1} is the generalization of the notion of critical point (when it is a local extremum point) of a one-dimensional map, and of the *fold curve* LC_{-1} of a two-dimensional noninvertible map.

From the definition given above it is clear that the relation $CS = T(CS_{-1})$ holds, and the points of CS_{-1} in which the map is continuously differentiable are necessarily points where the Jacobian determinant of T, denoted by $\det DT$, vanishes:

$$CS_{-1} \subseteq J_0 = \{p \in \mathbb{R}^n \mid \det DT(p) = 0\} \tag{2.6}$$

In fact, in any neighborhood of a point of CS_{-1} there are at least two distinct points which are mapped by T in the same point. Accordingly, the map is not locally invertible in points of CS_{-1}, and (2.6) follows from the implicit function theorem.

In order to explain the geometric meaning of the critical sets, let us consider a portion of CS, say $\widehat{CS}$, which separates two regions Z_k and Z_{k+2} of the phase space S, and let $\widehat{CS}_{-1}$ be the corresponding locus of merging preimages, i.e. $\widehat{CS} = T\left(\widehat{CS}_{-1}\right)$. This means that two inverses of T exist, say T_1^{-1} and T_2^{-1}, which are defined in the region Z_{k+2} (and have respective ranges in the regions R_1 and R_2 separated by $\widehat{CS}_{-1}$) that merge on $\widehat{CS}_{-1}$ (i.e. they give merging preimages on $\widehat{CS}_{-1}$) and no longer exist in the region Z_k. Now, let $U \subset S$ be a ball which intersects $\widehat{CS}_{-1}$ in $D = U \cap \widehat{CS}_{-1}$. Then $T(D) \subseteq \widehat{CS}$, and $T(U)$ is "folded" along $\widehat{CS}$ into the region Z_{k+2}. In fact, considering the two portions of U separated by $\widehat{CS}_{-1}$, say $U_1 \in R_1$ and $U_2 \in R_2$, we have that $T(U_1) \cap T(U_2)$ is a nonempty set included in the region Z_{k+2}, which is the region whose points p' have *rank-1* preimages $p_1 = T_1^{-1}(p') \in U_1$ and $p_2 = T_2^{-1}(p') \in U_2$. This means that two points $p_1 \in U_1$ and $p_2 \in U_2$, located at opposite sides with respect to

[1]This terminology, and notation, originates from the notion of critical points as it is used in the classical works of Julia and Fatou.

$\widehat{CS}_{-1}$, are mapped in the same side with respect to $\widehat{CS}$, in the region Z_{k+2}. This is also expressed by saying that the ball U is "folded" by T along CS on the side with more preimages (see Figure 1, obtained by the noninvertible map (2.11)). The same concept can be equivalently expressed by stressing the "unfolding" action of T^{-1}, obtained by the application of the two distinct inverses in Z_{k+2} which merge along CS. Indeed, if we consider a ball $V \subset Z_{k+2}$, then the set of its *rank-1* preimages $T_1^{-1}(V)$ and $T_2^{-1}(V)$ is made up of two balls $T_1^{-1}(V) \in R_1$ and $T_2^{-1}(V) \in R_2$. These balls are disjoint if $V \cap \widehat{CS} = \emptyset$ (Figure 1b).

It is worth to notice that in the case of piecewise differentiable maps the set of points where the map is not differentiable may belong to CS_{-1}, i.e. the images by T of such points may separate regions characterized by a different number of *rank-1* preimages (see e.g. Mira, 1987). For example, in one-dimensional continuous piecewise differentiable maps critical points may be located at the kinks where local maxima and minima are formed by two branches that join with slopes of opposite sign, such as the well known tent map or other piecewise linear maps. Moreover, piecewise continuous maps may have points of CS_{-1} at the discontinuities and, differently from the case of continuous maps, the corresponding portions of CS may separate regions that differ by an odd number of preimages (see again Mira, 1987). In any case, the importance of the set CS lies in the fact that its points separate regions Z_k characterized by different number of preimages[2].

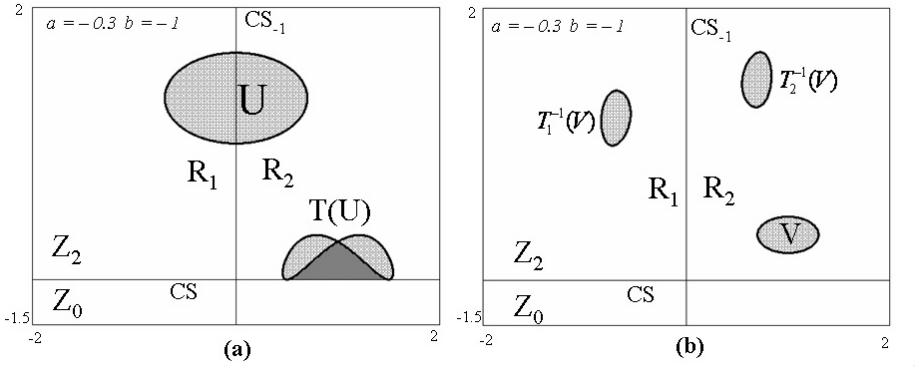

Figure 1.

2.1 Some examples in dimension one and two

As a first illustration, we consider a one-dimensional quadratic map, the logistic map (Figure 2a)

$$x' = f(x) = \mu x(1 - x). \tag{2.7}$$

[2]This property may also be shared by points where some inverses are not defined due to a vanishing denominator, as shown in Bischi et al., 1999b, 2003c.

This map has a unique critical point $c = \mu/4$, which separates the real line into the two subsets: $Z_0 = (c, +\infty)$, where no inverses are defined, and $Z_2 = (-\infty, c)$, whose points have two *rank-1* preimages. These preimages can be computed by the two inverses

$$x_1 = f_1^{-1}(x') = \frac{1}{2} - \frac{\sqrt{\mu\,(\mu - 4x')}}{2\mu}; \quad x_2 = f_2^{-1}(x') = \frac{1}{2} + \frac{\sqrt{\mu\,(\mu - 4x')}}{2\mu}. \tag{2.8}$$

If $x' \in Z_2$, its two *rank-1* preimages, computed according to (2.8), are located symmetrically with respect to the point $c_{-1} = 1/2 = f_1^{-1}(\mu/4) = f_2^{-1}(\mu/4)$. Hence, c_{-1} is the point where the two merging preimages of c are located. As the map (2.7) is differentiable, at c_{-1} the first derivative vanishes[3].

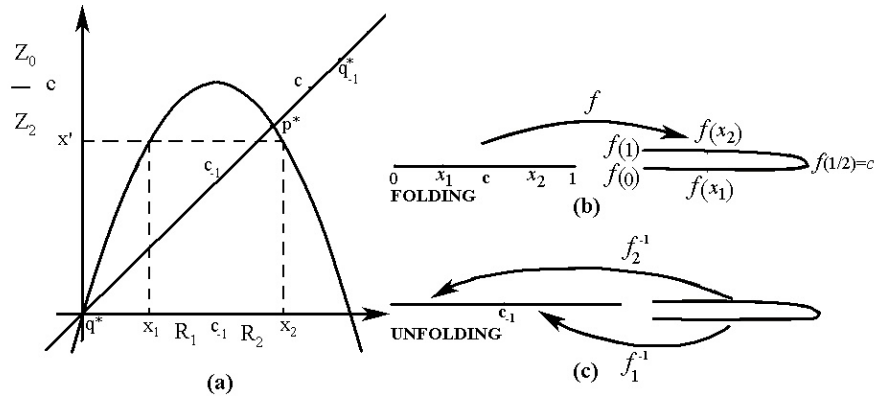

Figure 2.

In order to explain the geometric action of a critical point in a continuous map, let us consider again the logistic map and notice that as x moves from 0 to 1 the corresponding image $f(x)$ spans the interval $[0, c]$ twice, the critical point c being the turning point. In other words, if we consider how the segment $\gamma = [0, 1]$ is transformed by the map f we can say that it is *folded and pleated* to obtain the image $\gamma' = [0, c]$. Such folding gives

[3]We remark that in general the condition of vanishing derivative is not sufficient to define c_{-1}, since such condition may be also satisfied by points which are not local extrema (e.g. the inflection points with horizontal tangent).

a geometric reason why two distinct points of γ, say x_1 and x_2, located symmetrically with respect to the point $c_{-1} = 1/2$, are mapped into the same point $x' \in \gamma'$ (see Figure 2b). The same arguments can be explained by looking at the two inverse mappings f_1^{-1} and f_2^{-1} defined in $(-\infty, \mu/4]$ according to (2.8). We can consider the range of the map f formed by the superposition of two half-lines $(-\infty, \mu/4]$, joined at the critical point $c = \mu/4$ (Figure 2c), and on each of these half-lines a different inverse is defined. In other words, instead of saying that two distinct maps are defined on the same half-line we say that the range is formed by two distinct half lines on each of which a unique inverse map is defined. This point of view gives a geometric visualization of the definition of the critical point c as the point in which two distinct inverses merge. The action of the inverses, say $f^{-1} = f_1^{-1} \cup f_2^{-1}$, causes an unfolding of the range by mapping c into c_{-1} and by opening the two half-lines one on the right and one on the left of c_{-1}, so that the whole real line $\mathbb{R}$ is covered. So, the map f folds the real line, the two inverses unfold it (see Figure 2).

Another interpretation of the folding action of the unimodal map f is the following. Since $f(x)$ is increasing for $x \in [0, 1/2)$ and decreasing for $x \in (1/2, 1]$, its application to a segment $\gamma_1 \subset [0, 1/2)$ is orientation preserving, whereas its application to a segment $\gamma_2 \subset (1/2, 1]$ is orientation reversing. This suggests that an application of f to a segment $\gamma_3 = [a, b]$ including the point $c_{-1} = 1/2$ preserves the orientation of the portion $[a, c_{-1}]$, i.e. $f([a, c_{-1}]) = [f(a), c]$, whereas it reverses the portion $[c_{-1}, b]$, i.e. $f([c_{-1}, b]) = [f(b), c]$, so that $\gamma_3' = f(\gamma_3)$ is folded.

Let us now consider the case of a continuous two-dimensional map $T : S \to S$, $S \subseteq \mathbb{R}^2$, defined by

$$T : \begin{cases} x_1' = T_1(x_1, x_2) \\ x_2' = T_2(x_1, x_2) \end{cases}, \tag{2.9}$$

If we solve the system of the two equations (2.9) with respect to the unknowns x_1 and x_2, then, for a given (x_1', x_2'), we may have several solutions, representing *rank-1* preimages (or backward iterates) of (x_1', x_2'), say $(x_1, x_2) = T^{-1}(x_1', x_2')$, where T^{-1} is in general a multivalued relation.

In this case we say that T is noninvertible and the critical set, formed by critical curves LC (from the French "Ligne Critique"), constitutes the set of boundaries that separate regions of the plane characterized by a different number of *rank-1* preimages. Along LC at least two inverses give merging preimages, located on the set denoted by LC_{-1} , following the notations of Gumowski and Mira, 1980, Mira et al., 1996.

For a continuous and (at least piecewise) differentiable noninvertible map of the plane, the set LC_{-1} is included in the set where the Jacobian determinant $\det DT(x_1, x_2)$ changes sign, since T is locally an orientation preserving map near points (x_1, x_2) such that $\det DT(x_1, x_2) > 0$ and orientation reversing if $\det DT(x_1, x_2) < 0$. Of course, $LC = T(LC_{-1})$.

In order to understand this point, let us recall that when an affine transformation $x' = Ax + b$, where $A = \{a_{ij}\}$ is a 2×2 matrix and $b \in \mathbb{R}^2$, is applied to a figure of the plane, then the area of the transformed figure grows, or shrinks, by a factor $\rho = |\det A|$, and if $\det A > 0$ then the orientation of the figure is preserved, whereas if $\det A < 0$ then the orientation is reversed. This property also holds for the linear approximation of (2.9)

in a neighborhood of a point $p = (x_1, x_2)$, given by an affine map with $A = DT$, DT being the Jacobian matrix evaluated at the point p

$$DT\,(p) = \begin{bmatrix} \partial T_1/\partial x_1 & \partial T_1/\partial x_2 \\ \partial T_2/\partial x_1 & \partial T_2/\partial x_2 \end{bmatrix} \tag{2.10}$$

A qualitative visualization is given in Figure 3a.

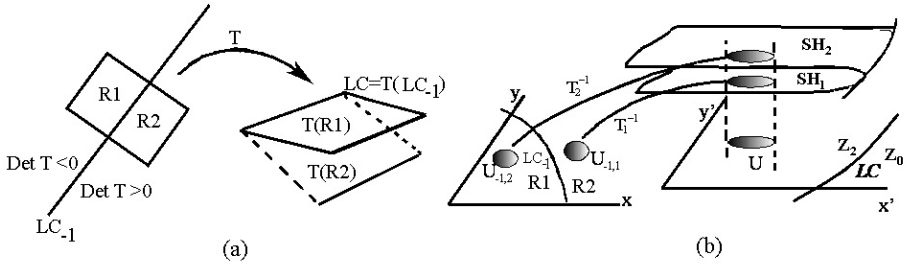

Figure 3.

In order to give a geometrical interpretation of the action of a multi-valued inverse relation T^{-1}, it is useful to consider a region Z_k as the superposition of k sheets, each associated with a different inverse. Such a representation is known as *Riemann foliation* of the plane (see Mira et al., 1996). Different sheets are connected by folds, and the projections of such folds on the phase plane are arcs of LC. This is shown in the qualitative sketch of Figure 3b, where the case of a $Z_0 - Z_2$ noninvertible map is considered. This graphical representation of the unfolding action of the inverses gives an intuitive idea of the mechanism which causes the creation of nonconnected basins for noninvertible maps of the plane.

To give an example, let us again consider a quadratic map $T : (x, y) \to (x', y')$, extensively studied in Mira et al., 1996, and Abraham et al., 1997, defined by

$$T : \begin{cases} x' = ax + y \\ y' = b + x^2 \end{cases} \tag{2.11}$$

Given x' and y', if we try to solve the algebraic system with respect to the unknowns x and y we get two solutions, given by

$$T_1^{-1}: \begin{array}{l} x = -\sqrt{y'-b} \\ y = x' + a\sqrt{y'-b} \end{array} \quad ; \qquad T_2^{-1}: \begin{array}{l} x = \sqrt{y'-b} \\ y = x' - a\sqrt{y'-b} \end{array} \tag{2.12}$$

if $y' \geq b$, and no solutions if $y' < b$. So, (2.11) is a $Z_0 - Z_2$ noninvertible map, where Z_0 (region whose points have no preimages) is the half plane $Z_0 = \{(x,y)\,|y < b\}$ and Z_2 (region whose points have two distinct *rank-1* preimages) is the half plane $Z_2 = \{(x,y)\,|y > b\}$. The line $y = b$, which separates these two regions, is LC, and the locus LC_{-1} of points having two merging *rank-1* preimages is located on the line $x = 0$ (see Figure 1). Being (2.11) a continuously differentiable map, the points of LC_{-1} necessarily belong to the set of points at which the Jacobian determinant vanishes, i.e. $LC_{-1} \subseteq J_0$, where $J_0 = \{(x,y)\,|\det DT(x,y) = -2x = 0\}$. In this case LC_{-1} coincides with J_0 (the vertical axis $x = 0$) and the critical curve LC is the image by T of LC_{-1}, i.e. $LC = T(LC_{-1}) = T(\{x = 0\}) = \{(x,y)\,|y = b\}$.

As stressed above, a study of the basins of attraction of a map T requires a global analysis of the properties of its inverses. In particular, if T is a noninvertible map, complicated topological structures of the basins, such as nonconnected sets (i.e. formed by many disjoint portions) and/or sets with fractal boundaries, are often observed[4].

The route to more and more complex basin boundaries, as some parameter is varied, is characterized by global bifurcations, also called *contact bifurcations*, due to contacts between the critical set and the basins' boundaries. Some particular examples in dimension one and two will be given below. However, the origin of complex topological structures of the basins, like those formed by nonconnected sets, can be heuristically explained on the basis of the geometrical properties of a noninvertible map. For example, suppose that p is a fixed point of T. Since $T(p) = p$, one of the preimages of p is p itself, but if T^{-1} is multivalued. in p, i.e. $p \in Z_k$ with $k \geq 2$, then other preimages of the fixed point p exist. If the fixed point is stable, and $U(p)$ is a neighborhood of p that belongs to its basin of attraction, then the basin of p must also include all the *rank-1* preimages of the points of $U(p)$, which may be disjoint from $U(p)$, due to the unfolding action of the inverses defined in $U(p)$ (see Figure 3b). Moreover, if also such disjoint preimages belong to regions where some inverses exist, higher rank preimages of $U(p)$ belong to the basin of p, and so on. This may give rise to a so called "arborescent sequence" of (countable) infinitely many nonconnected portions of the basin.

Hence if a parameter variation causes a crossing between a basin boundary and a critical set which separates different regions Z_k, so that a portion of a basin enters a region where an higher number of inverses is defined, then new components of the basin may suddenly appear at the contact. This is the basic mechanism which causes the creation of more and more complex structures of the basins, as we shall see in the examples given in the following sections.

[4]For the map (2.11) several studies and graphical representations of the basins and their qualitative changes are given in Mira et al., 1994, Mira and Rauzy, 1995, Mira et al., 1996, Abraham et al., 1997.

3 Basin boundaries and contact bifurcations in one-dimensional noninvertible maps

In this section, we consider continuous one-dimensional maps. Before describing the contact bifurcations, let us take a look at iterated invertible maps. If $f : I \to I$ is a continuous and increasing function, then the only invariant sets are the fixed points. When many fixed points exist, say $x_1^* < x_2^* < ... < x_k^*$, they are alternatively stable and unstable: the unstable fixed points are the boundaries that separate the basins of the stable ones (see Figure 4a). Starting from an initial condition where the graph of f is above the diagonal, i.e. $f(x_0) > x_0$, the generated trajectory is an increasing sequence converging to the stable fixed point on the right. Starting from an initial condition such that $f(x_0) < x_0$, the trajectory is a decreasing sequence converging to the fixed point on the left (see Figure 4a, where p^* is a stable fixed point, and its basin is bounded by two unstable fixed points q^* and r^*, with $q^* < p^* < r^*$). If $f : I \to I$ is a continuous and decreasing map, the only possible invariant sets are one fixed point and cycles of period 2. In fact f^2 can only have fixed points (since $f^2 = f \circ f$ is an increasing map), that include the fixed points of f and periodic points of period 2 of f. The periodic points of the 2-cycles must be located at opposite sides with respect to the unique fixed point, the unstable ones being boundaries of the basins of the stable ones (see Figure 4b, where a stable fixed point x^* exists, and its basin is bounded by the periodic points α_1, α_2 of an unstable cycle of period 2). If the fixed point x^* is stable and no cycles exist, then x^* is globally stable.

So, if the map is invertible, the basins of the attracting sets have always quite simple structures: for stable fixed points they are formed by a unique open interval that includes the fixed point, for stable two cycles they are formed by two open intervals each one including one periodic point. In general, this is not true if the map is noninvertible. In fact, in this case nonconnected portions of the basins may exist, given by open intervals that do not include any point of the related attractor.

As a first example, let us consider the logistic map (2.7), that is, as we showed, a noninvertible $Z_0 - Z_2$ map whose graph is represented again in Figure 5. For $\mu < 4$ every initial condition $x_0 \in (0, 1)$ generates bounded sequences, converging to a unique attractor A[5], whereas initial conditions out of the interval $[0, 1]$ generate sequences diverging to (minus) infinity. The boundary that separates the basin of the attractor A, $\mathcal{B}(A)$, from the basin of diverging trajectories, $\mathcal{B}(\infty)$ - marked by bold lines in Figure 5a - , is formed by the unstable fixed point $q^* = 0$ and its *rank-1* preimage (different from itself), $q_{-1}^* = 1$. Observe that, of course, a fixed point is always preimage of itself, but in this case also another preimage exists because $q^* \in Z_2$. If $\mu < 4$, like in Figure 5a, $q_{-1}^* > c = \mu/4$, where c is the critical point (maximum) that separates Z_0 and Z_2. Hence, $q_{-1}^* \in Z_0$, and consequently no preimages of higher order exist. If we increase μ, at $\mu = 4$ we have $q_{-1}^* = c = 1$, and a contact between the critical point and the basin boundary occurs. This is a global bifurcation, which changes the structure of the basin. For $\mu > 4$, we have $q_{-1}^* < c$, and the portion $\left(q_{-1}^*, c\right)$ of $\mathcal{B}(\infty)$ enters Z_2. This implies that new

[5]The attractor A may be the fixed point $x^* = (\mu - 1)/\mu$ or a more complex attractor, periodic or chaotic, located around x^*, see Devaney, 1987.

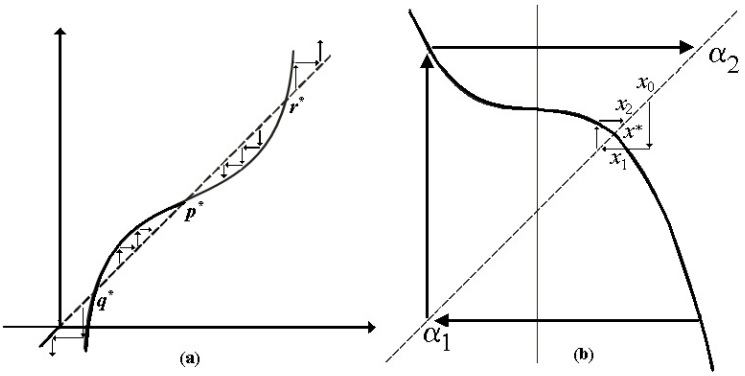

Figure 4.

preimages of that portion are created, which belong to $\mathcal{B}(\infty)$ according to (2.4). The two *rank-1* preimages of $\left(q_{-1}^{*}, c\right)$ are located in a neighborhood I_0 of the critical point $c_{-1} = 1/2$, as shown in Figure 5b. Points of I_0 exit the interval $(0, 1)$ after one iteration, thus giving unbounded sequences. As $I_0 \in Z_2$, it also has two *rank-1* preimages, that are *rank-2* preimages of $\left(q_{-1}^{*}, c\right)$. These preimages are given by the two smaller intervals denoted by $I_{-1}^{(1)}$ and $I_{-1}^{(2)}$ in Figure 5b, and are located symmetrically with respect to $c_{-1} = 1/2$. Points belonging to $I_{-1}^{(1)}$ and $I_{-1}^{(2)}$ exit the interval $(0, 1)$ after two iterations of (2.7). Even these two smaller – nonconnected – portions of $\mathcal{B}(\infty)$ are in Z_2. Hence, each of them has two preimages, which again result in nonconnected portions of $\mathcal{B}(\infty)$. Obviously, this process gives rise to a infinite sequence of preimages whose points generate unbounded sequences. So, after the contact between the critical point c and the basin boundary q_{-1}^{*}, infinitely many nonconnected portions of $\mathcal{B}(\infty)$ are created inside $(0, 1)$ (only a few of them are shown in Figure 5b). The union of all these preimages is an open set whose closure is $[0, 1]$. Its complement in $[0, 1]$ has zero Lebesgue measure and is a Cantor set (see Guckenheimer and Holmes, 1983, Devaney, 1987). After this bifurcation the attractor at finite distance no longer exists, and the generic trajectory is divergent. This global bifurcation is called *final bifurcation* in Mira et al., 1996 or in Abraham et al., 1997, and *boundary crisis* in Grebogi et al., 1983.

A similar situation occurs for a unimodal $Z_0 - Z_2$ map where the attractor at infinity

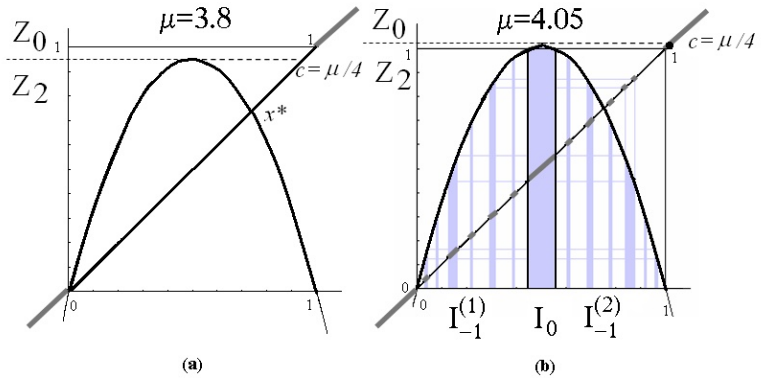

Figure 5.

is replaced by an attracting fixed point, like the one shown in Figure 6. As in the previous example, we have an attractor A, which may be the fixed point x^* (or some other invariant set around it), with a simply connected basin bounded by the unstable fixed point q^* and its *rank-1* preimage q^*_{-1}. Note that in this case, differently from the previous one, initial conditions taken in the complementary of $\mathcal{B}(x^*)$ generate trajectories converging to the stable fixed point z^*. This means that the basin $\mathcal{B}(z^*)$ is formed by the union of two nonconnected portions: $B_0 = (-\infty, q^*) \subset Z_2$, a connected set containing z^* called *immediate basin*, and $B_1 = \left(q^*_{-1}, +\infty\right) = f^{-1}(B_0) \subset Z_0$. In Figure 6 the two nonconnected portions of the basin $\mathcal{B}(z^*)$ are marked by bold lines. Now suppose that some parameter variation makes the critical point c (maximum value) increase until it crosses the basin boundary q^*_{-1}. Then the interval (q^*_{-1}, c), which is part of B_1, enters Z_2, and infinitely many nonconnected portions of $\mathcal{B}(z^*)$ emerge in the interval (q^*, q^*_{-1}). Note that the total basin can still be expressed as the union of all the preimages of any rank of the immediate basin B_0, and the boundary $\partial\mathcal{B}(z^*)$ is the set of infinitely many preimages of any rank of q^*.

Changing the right branch of the map depicted in Figure 6 by folding it upwards, another critical point (a minimum) is created (Figure 7). This map is now a $Z_1 - Z_3 - Z_1$ noninvertible map, where Z_3 is the portion of the codomain bounded by the relative minimum value $c_{\min}$ and relative maximum value $c_{\max}$. In the Figure 7a we have three

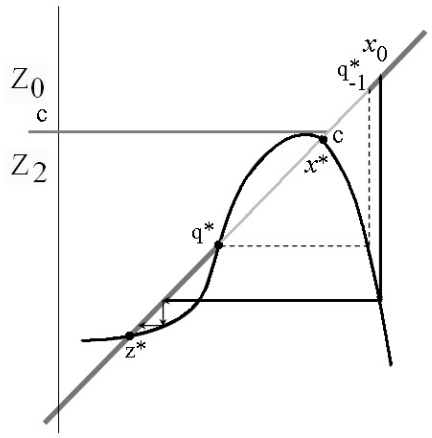

Figure 6.

attractors: the fixed point z^*, with $\mathcal{B}(z^*) = (-\infty, q^*)$, the attractor A around x^*, with basin $\mathcal{B}(A) = (q^*, r^*)$ bounded by two unstable fixed points, and $+\infty$ (i.e. positively diverging trajectories) with basin $\mathcal{B}(+\infty) = (r^*, +\infty)$. In this case all the basins are immediate, each given by an open interval. Both basin boundaries q^* and r^* are in Z_1, so they are the only preimages of themselves (like for an invertible map). However, the situation drastically changes if the minimum value $c_{\min}$ moves downwards below q^* (as in Figure 7b). After the global bifurcation, when $c_{\min} = q^*$, the portion $(c_{\min}, q^*)$ enters Z_3, so new preimages $f^{-k}(c_{\min}, q^*)$ appear with $k \geq 1$. These preimages constitute an infinite (countable) set of nonconnected portions (or *holes*) of $\mathcal{B}(z^*)$ nested inside $\mathcal{B}(A)$, represented by the thick portions of the diagonal in Figure 7b, bounded by the infinitely many preimages of any rank, say q^*_{-k}, $k \in \mathbb{N}$, of q^*, that accumulate in a left neighborhood of the fixed point r^*. In fact, as r^* is a repelling fixed point for the forward iteration of f, it is an attracting fixed point for the backward iteration of the same map.

To conclude, we stress that in the context of noninvertible maps it is useful to define the *immediate basin* $\mathcal{B}_0(A)$, of an attracting set A, as the widest connected component of the basin which contains A. Then the total basin can be expressed as $\mathcal{B}(A) = \bigcup_{n=0}^{\infty} T^{-n}(\mathcal{B}_0(A))$.

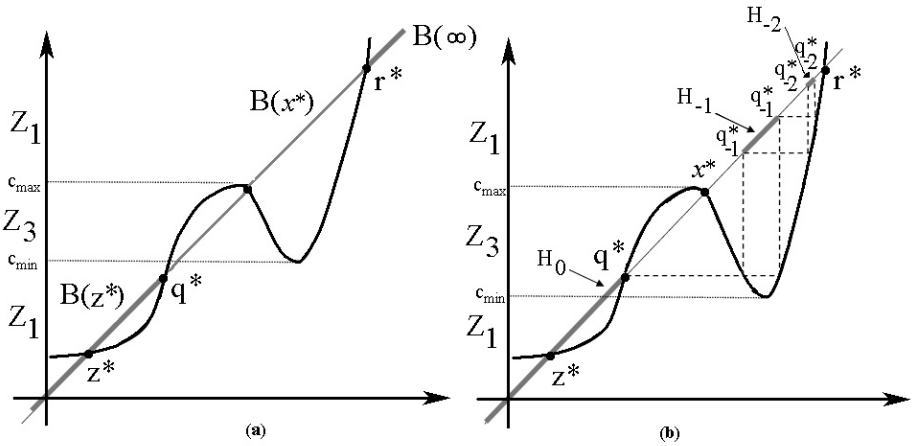

Figure 7.

The previous example shows that a contact between a critical point and a basin boundary marks the transition from simple connected to nonconnected basins: infinitely many nonconnected portions are suddenly created, given by the preimages of any rank of the portion H_0 of $\mathcal{B}(z^*)$ included into Z_3, say $H_{-i} = T^{-i}(H_0)$, $i = 1, 2, ...$

Several examples where the multiplicity of preimages leads to basins with complex structures are given on Mira et al., 1994, Mira and Rauzy, 1995, Mira et al., 1996, chap. 5, Abraham et al., 1997, Bischi et al., 2003a,b[6], Bischi et al., 2004).

To conclude this section, we briefly describe a unimodal map, i.e. a map with a unique critical point c which separates Z_0 from Z_2, with two inflection points, like in the graphs shown in Figure 8 (this example is taken from Gumowski and Mira, 1980).

This map has four fixed points, $q < s < r < p$, with q and r unstable and s stable. The fixed point p belongs to the trapping interval $R = [r, r_{-1}]$ and the restriction of the map to R behaves like a logistic map. In Figure 8 three attractors are present: the infinity, the stable fixed point s and the attractor I included inside the absorbing

[6]Where an evolutionary game is studied, described by the map

$$x(t+1) = x(t) + x(t)(1 - x(t))\frac{2}{\pi}\arctan\left[\frac{\lambda\pi}{2}\left(A - B(x_{1,t}+1) - \frac{C}{1+\beta x_{1,t}}\right)\right]$$

whose graph is very similar to the one shown in fig. 7.

interval R, which may be the fixed point p, a cycle around it or a chaotic attractor. The respective basins are:

$$\mathcal{B}(\infty) = (-\infty, q) \cup (q_{-1}, +\infty) \qquad \mathcal{B}(s) = (q, r) \cup (r_{-1}, q_{-1}); \qquad \mathcal{B}(I) = (r, r_{-1});$$

If the critical point c moves upwards as a parameter is varied, when $c = r_{-1}$ the final bifurcation (or boundary crisis) of the invariant interval R occurs, and for $c > r_{-1}$ the interval R is no longer invariant because the portion (r_{-1}, c) of $\mathcal{B}(s)$ enters R, as well as its infinitely many preimages. In fact, after this contact, the segment (r_{-1}, c) of $\mathcal{B}(s)$ belongs to Z_2 and infinitely many "holes" of $\mathcal{B}(s)$ are created inside R, given by the preimages of any rank of (r_{-1}, c). Inside R only a chaotic repellor, given by a zero-measure Cantor set Λ, survives, and the generic trajectory with initial condition $x_0 \in (q, q_{-1})$ tends to the fixed point s. Thus, after the contact bifurcation, the basin $\mathcal{B}(s)$ has a fractal boundary because besides the outer boundary, given by the points q and q_{-1} which separate it from $\mathcal{B}(\infty)$, also the points of Λ belong to the boundary of $\mathcal{B}(s)$. As c further increases, another global bifurcation occurs when $c = q_{-1}$. After this bifurcation the portion (q_{-1}, c) of $\mathcal{B}(\infty)$ enters Z_2 and infinitely many preimages of it enter inside R. These constitute a set of infinitely many holes of $\mathcal{B}(\infty)$ nested inside $\mathcal{B}(s)$. At this stage, two sets of positive measure, made up of infinitely many disjoint subsets of $\mathcal{B}(\infty)$ and $\mathcal{B}(s)$, are nested inside R: In fact, both $(q_{-1}, c) \in \mathcal{B}(\infty)$ and $(r_{-1}, q_{-1}) \in \mathcal{B}(s)$ are inside Z_2 and have infinitely many preimages inside R. The boundary which separates $\mathcal{B}(s)$ and $\mathcal{B}(\infty)$ inside R is the chaotic repeller Λ (see Mira et al., 1996 for a more detailed discussion of this example). The above discussion has only been based on qualitative consideration related to a graph, without any analytic representation of the function. The simplest map whose graph has a shape similar to the one shown in Figure 8 is a quartic map (i.e. a polynomial of degree 4) which has only a critical point (i.e. $f'(x)$ is a cubic polynomial with only one real root) and two inflection points (i.e. $f''(x)$ is a quadratic polynomial with two real roots). An example of a map having such properties is $x' = f(x) = x(1-x)\left(\mu x^2 + (4-\mu)x + 3\right)$. As μ is increased, all the situations described above are obtained (an exercise left to the reader).

4 Basin boundaries and their bifurcations in two-dimensional noninvertible maps

As shown for one dimensional maps, even for higher dimensional maps the global bifurcations that lead to basins formed by nonconnected sets can be explained in terms of contacts between basins boundaries and critical sets. We now consider some examples, taken from recent models of economic dynamics, where two-dimensional iterated maps are used to describe the interaction among economic agents. In these examples we stress that the route to more and more complex basin boundaries, as some parameter is varied, is characterized by global bifurcations due to contacts between critical curves and the invariant sets that constitute the basins' boundaries in two-dimensional maps, such as the stable sets of saddle points or cycles, or unstable closed invariant orbits.

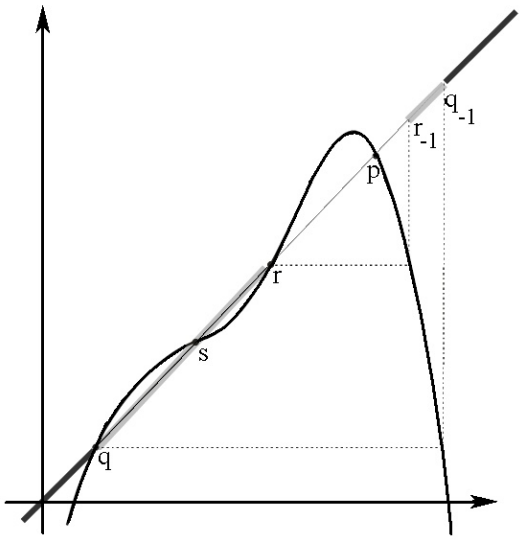

Figure 8.

For two-dimensional maps, such kinds of bifurcations can be very rarely studied by analytical methods, since the analytical equation of a singularity is not known in general. Hence the analysis is mainly performed by geometrical and numerical methods.

4.1 A Cournot duopoly game with best reply, naive expectations and adaptive behavior

We consider a Cournot duopoly game where at each time period t two firms decide their next period productions on the basis of *best reply* functions expressed as $q_i(t+1) = r_i(q_j(t))$, $i, j = 1, 2$, $i \neq j$. We assume that competitors exhibit some kind of inertia, adjusting their previous production quantities in the direction of the Best Response, according to the following adjustment mechanism

$$\begin{aligned} q_1(t+1) &= q_1(t) + \lambda_1 \left(r_1(q_2(t)) - q_1(t)\right) \\ q_2(t+1) &= q_2(t) + \lambda_2 \left(r_2(q_1(t)) - q_2(t)\right) \end{aligned} \tag{4.1}$$

where the parameters $\lambda_i \in [0, 1]$, $i = 1, 2$, represent the *speeds of adjustment*. Following Kopel, 1996, we assume in (4.1) reaction functions in the form of logistic maps $r_i(q_j) = \mu_i q_j (1 - q_j)$, so that the time evolution of the game is obtained by the iteration of the

two-dimensional map $T : (q_1, q_2) \to (q_1', q_2')$ defined by

$$T : \begin{cases} q_1' = T_1(q_1, q_2) = (1 - \lambda_1)\, q_1 + \lambda_1 \mu_1 q_2\, (1 - q_2) \\ q_2' = T_2(q_1, q_2) = (1 - \lambda_2)\, q_2 + \lambda_2 \mu_2 q_1\, (1 - q_1) \end{cases} . \tag{4.2}$$

The fixed points of map (4.2), located at the intersections of the two reaction curves, coincide with the Nash equilibria of the duopoly game (see again Kopel, 1996). If we assume that $\mu_1 = \mu_2 = \mu$, the fixed points can be expressed by simple analytical expressions: besides $O = (0, 0)$ we have $S = \left(1 - \frac{1}{\mu}, 1 - \frac{1}{\mu}\right)$, that for $\mu > 1$ represents a symmetric Nash equilibrium, since it is characterized by identical quantities of the two firms. Two further Nash equilibria, given by

$$E_1 = \left(\frac{\mu + 1 + \sqrt{(\mu + 1)\,(\mu - 3)}}{2\mu}, \frac{\mu + 1 - \sqrt{(\mu + 1)\,(\mu - 3)}}{2\mu} \right) \tag{4.3}$$

and

$$E_2 = \left(\frac{\mu + 1 - \sqrt{(\mu + 1)\,(\mu - 3)}}{2\mu}, \frac{\mu + 1 + \sqrt{(\mu + 1)\,(\mu - 3)}}{2\mu} \right), \tag{4.4}$$

are created at $\mu = 3$. For $\mu > 3$ they are located in symmetric positions with respect to the diagonal Δ of equation $q_1 = q_2$. Each of them represents a nonsymmetric Nash equilibrium: In E_1 firm 1 produces more than firm 2 in exactly the same way as firm 2 produces more than firm 1 in E_2. A study of the local stability of the equilibria reveals that O is stable for $\mu < 1$, S is stable for $1 < \mu < 3$ and for $\mu > 3$ a range of parameters μ, λ_1, λ_2 exists such that S is a saddle point and E_i, $i = 1, 2$, are both stable. Moreover, the map (4.2) can generate diverging trajectories, that is, an attractor at infinite distance exists (see Bischi and Kopel, 2001). This naturally leads to the question of the delimitation of the basins of attraction. Numerically computed basins of attraction are shown in Figures 10 and 11, where the dark grey region represents $\mathcal{B}(\infty)$, and the complementary set is subdivided into the basins of the stable Nash equilibria E_1 and E_2, represented by white and light grey regions respectively. These Figures show that the structure of the basins may be quite different as the values of the parameters vary, and we try to understand the basic mechanisms that cause such qualitative changes.

As argued in the previous sections, a study of the inverses of the map become important in order to understand the structure of the basins and their qualitative changes. Indeed, the map (4.2) is a noninvertible map, because given a point $q' = (q_1', q_2') \in \mathbb{R}^2$ its *rank-1* preimages $T^{-1}(q')$ may be more than one, i.e., T^{-1} is a multivalued relation. Such preimages can be computed by solving the following algebraic system obtained from (4.2) with respect to the quantities q_1 and q_2:

$$\begin{cases} (1 - \lambda_1) q_1 + \lambda_1 \mu_2 q_2 (1 - q_2) = q_1' \\ (1 - \lambda_2) q_2 + \lambda_2 \mu_1 q_1 (1 - q_1) = q_2' \end{cases} \tag{4.5}$$

This is a fourth degree algebraic system, which may have four, two or no real solutions. According to the number of distinct *rank-1* preimages associated with each point of $\mathbb{R}^2$,

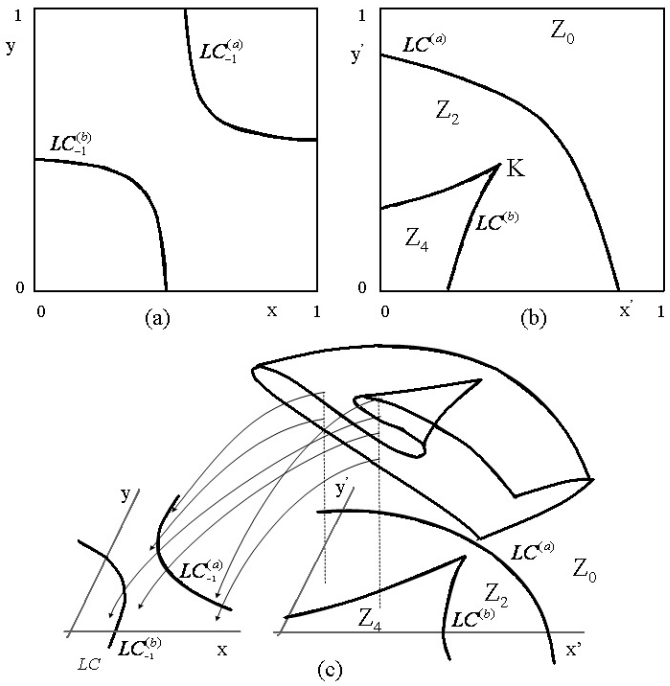

Figure 9.

the plane can be subdivided into regions, denoted by Z_k, $k = 0, 2, 4$, whose points have k distinct preimages, hence the map (4.2) is a noninvertible map of $Z_0 - Z_2 - Z_4$ type.

Being (4.2) a continuously differentiable map, the set LC_{-1} belongs to the set of points in which the Jacobian determinant vanishes, which can be computed by solving the equation

$$\left(q_1 - \frac{1}{2}\right)\left(q_2 - \frac{1}{2}\right) = \frac{(1-\lambda_1)(1-\lambda_2)}{4\lambda_1\lambda_2\mu_1\mu_2} \tag{4.6}$$

This equation represents an equilateral hyperbola, whose two branches are denoted by $LC_{-1}^{(a)}$ and $LC_{-1}^{(b)}$ in Figure 9a. It follows that also $LC = T(LC_{-1})$ is the union of two branches, say $LC^{(a)} = T(LC_{-1}^{(a)})$ and $LC^{(b)} = T(LC_{-1}^{(b)})$. $LC^{(a)}$ separates the region Z_0, whose points have no preimages, from the region Z_2, whose points have two distinct *rank-1* preimages. $LC^{(b)}$ separates the region Z_2 from Z_4, whose points have four distinct preimages (see Figure 9b). Notice that any point of $LC^{(a)}$ has two coincident *rank-1* preimages which are located at a point of $LC_{-1}^{(a)}$, and any point of $LC^{(b)}$ has two coincident *rank-1* preimages which are located at a point of $LC_{-1}^{(b)}$ plus two further distinct *rank-1* preimages, called *extra preimages* (see e.g. Mira et al. 1996). The

Riemann foliation associated with the map (4.2) is qualitatively represented in Figure 9c. It can be noticed that a cusp point of LC exists, denoted by K, characterized by three merging preimages at the junction of two folds.

The first task in order to gain some insight into the robustness of the model is the delimitation of the boundary that separates the basin of infinity, $\mathcal{B}(\infty)$, from the set of points that generate bounded (hence economically meaningful) trajectories, denoted by

$$\mathcal{B} = \mathbb{R}^2 \setminus \overline{\mathcal{B}(\infty)} \tag{4.7}$$

where $\overline{\mathcal{B}(\infty)} = \mathcal{B}(\infty) \cup \partial\mathcal{B}(\infty)$ is the closure of $\mathcal{B}(\infty)$. The boundary $\partial\mathcal{B} = \partial\mathcal{B}(\infty)$ behaves as a repelling set for the points near it, since it acts like a watershed for the trajectories of the map T. From (2.5) it follows that if an unstable fixed point or cycle belongs to $\partial\mathcal{B}$ then $\partial\mathcal{B}$ must also contain all of its preimages of any rank. Moreover, if a saddle-point, or a saddle-cycle, belongs to $\partial\mathcal{B}$, then $\partial\mathcal{B}$ must also contain the whole stable set (see Gumowski and Mira 1980, Mira et al. 1996). Let us first consider the case $\lambda_1 = \lambda_2 = \lambda$. For $\mu > 1$ and $0 < \lambda < 2/(\mu + 1)$ the fixed point O is a saddle (see Bischi and Kopel, 2001) with unstable set $W^u(O)$ reaching S along the diagonal Δ and local stable set $W^s_{loc}(O)$ crossing through O perpendicular to Δ. The stable set $W^s_{loc}(O) \subseteq \partial\mathcal{B}$. In fact, if we consider a neighborhood of O, $W^s_{loc}(O)$ is a separatrix between the trajectories which converge to a bounded attractor (generated by the points above $W^s_{loc}(O)$) and those which diverge to $-\infty$ (generated by the points below $W^s_{loc}(O)$, see Figure 10a). The boundary $\partial\mathcal{B}$ is given by the whole stable set $W^s(O)$, obtained by taking the preimages of any rank of $W^s_{loc}(O)$

$$\partial\mathcal{B} = W^s(O) = \bigcup_{k\geq 0} T^{-k}\left(W^s_{loc}(O)\right)$$

In the symmetric case of homogeneous players, i.e. $\mu_1 = \mu_2 = \mu$ and $\lambda_1 = \lambda_2 = \lambda$, the preimages of O can be analytically computed, and their coordinates allow us to obtain a rough estimate of the extension of $\mathcal{B}$. Indeed, the diagonal Δ is a trapping submanifold for the map T, i.e., $T(\Delta) \subseteq \Delta$[7]. The trajectories, embedded into the one-dimensional submanifold Δ, are governed by the restriction of the two-dimensional map T to Δ, $f = T|_\Delta : \Delta \to \Delta$, where the map f, which is obtained by setting $q_1 = q_2 = q$ and $q'_1 = q'_2 = q'$ in (4.2), is given by

$$q' = f(q) = (1 + \lambda(\mu - 1))\, q - \lambda\mu q^2 \tag{4.8}$$

So, if $O \in Z_2$ (like in Figure 10a) its two *rank-1* preimages are O itself (being O a fixed point) and

$$O^{(1)}_{-1} = \left(\frac{1 + \lambda(\mu - 1)}{\lambda\mu}, \frac{1 + \lambda(\mu - 1)}{\lambda\mu}\right) \in \Delta. \tag{4.9}$$

that can be computed by solving the equation (4.8) with $q' = 0$. The condition $O \in Z_2$ can be analytically determined because in the case of homogeneous players also the cusp

[7]This means nothing more than if two firms start with equal quantities $q_1(0) = q_2(0)$ and behave identically, then their choices will be the same for each future time period.

point K of LC_{-1} belongs to the diagonal Δ, and its coordinates can be analytically computed (see Bischi and Kopel, 2001):

$$K = LC^{(b)} \cap \Delta = (k, k) \quad \text{with} \quad k = \frac{(\lambda(\mu+1)-1)(\lambda\mu+3(1-\lambda))}{4\lambda\mu} \tag{4.10}$$

If $0 < \lambda < 1/(\mu+1)$ then $O \in Z_2$, otherwise $O \in Z_4$, i.e., it has four *rank-1* preimages (see Figure 10b). In this case, two of them, O and $O_{-1}^{(1)}$, belong to Δ, and the other two, say $O_{-1}^{(2)}$ and $O_{-1}^{(3)}$, are located in symmetric positions with respect to Δ and belong to the line Δ_{-1}, of equation $q_1 + q_2 = 1 + \frac{1}{\mu}\left(1 - \frac{1}{\lambda}\right)$. Indeed, the preimages of the points of Δ are located on Δ or on Δ_{-1}, as it can be seen by setting $q_1' = q_2'$ in (4.5) and adding or subtracting the two symmetric equations. In particular, with $q_1' = q_2' = 0$ we get the solution

$$O_{-1}^{(2)} = \left(\frac{\lambda(\mu+1)-1+\sqrt{\lambda^2\mu^2+2\lambda\mu(1-\lambda)-3(\lambda^2+1)+6\lambda}}{2\lambda\mu}, \right. \tag{4.11}$$
$$\left. \frac{\lambda(\mu+1)-1-\sqrt{\lambda^2\mu^2+2\lambda\mu(1-\lambda)-3(\lambda^2+1)+6\lambda}}{2\lambda\mu}\right)$$

and the symmetric solution $O_{-1}^{(3)}$ is obtained from $O_{-1}^{(2)}$ by swapping the two coordinates.

So, if $0 < \lambda < 1/(\mu+1)$, the stable set $W^s(O)$ consists of two smooth arcs connecting O and $O_{-1}^{(1)}$, symmetric with respect to Δ, as in Figure 10a. If $\lambda > 1/(\mu+1)$ then $W^s(O)$ has a similar shape, with the symmetric arcs connecting O and $O_{-1}^{(1)}$ which pass through the points $O_{-1}^{(2)}$ and $O_{-1}^{(3)}$, as shown in Figure 10b, obtained for $\mu = 3.4$ and $\lambda = 0.5$. It is also important to notice that even after the bifurcation occurring at $\lambda(\mu+1) = 2$, when O is transformed from a saddle point into an unstable node with the simultaneous creation of a saddle cycle C_2 of period 2, the boundary $\partial\mathcal{B}$ remains practically the same. In fact, in this case $\partial\mathcal{B} = \overline{W^s(C_2)}$, which continues to include O and its preimages of any rank.

The "size" of the basin $\mathcal{B}$ of bounded trajectories, as well as the influence of parameters λ and μ on it, can be estimated knowing the coordinates of O and $O_{-1}^{(1)}$. In fact, in the case of homogeneous behavior, the length of the segment $OO_{-1}^{(1)}$, given by $l(OO_{-1}^{(1)}) = \sqrt{2}\left[1+\lambda(\mu-1)\right]/\lambda\mu$ is a decreasing function of both parameters λ and μ, and it goes to infinity as $\lambda \to 0^+$, i.e. the basin of bounded trajectories tends to include the whole diagonal in such a limiting case. It is also interesting to note that in the other limiting case, $\lambda \to 1^-$, we get $O_{-1}^{(1)} \to (1,1)$, $O_{-1}^{(2)} \to (1,0)$, $O_{-1}^{(3)} \to (0,1)$. Hence in the case of instantaneous adjustment ($\lambda = 1$), the basin of the bounded trajectories becomes the square $(0,1)\times(0,1)$. This result also holds for $\mu_1 \neq \mu_2$, as proved in Bischi et al., 2000b.

Many of the arguments given above continue to hold in the case of different speeds of adjustment $\lambda_1 \neq \lambda_2$. However, a simple analytical expression of the preimages of O cannot be obtained, since in this case they are given by the solution of the fourth degree nonsymmetric algebraic system (4.5). The diagonal Δ is no longer invariant and the basins are no longer symmetric with respect to Δ.

Let us move now to the problem of the delimitation of the basins $\mathcal{B}(E_1)$ and $\mathcal{B}(E_2)$ of the two stable equilibria E_1 and E_2 respectively. The boundary of each of these two basins is formed by an "outer portion", which separates them from $\mathcal{B}(\infty)$, and an "inner portion", separating $\mathcal{B}(E_1)$ and $\mathcal{B}(E_2)$, which contains the saddle point S as well as its whole stable set $W^s(S)$. In fact, just after the pitchfork bifurcation, occurring at $\mu = 3$, at which the two stable fixed points E_1 and E_2 are created, the symmetric equilibrium $S \in \Delta$ is a saddle, provided that $0 < \lambda < \frac{2}{\mu-1}$, and the two branches of unstable set $W^u(S)$ departing from it reach the two stable nodes E_1 and E_2. Hence the local stable set $W^s_{loc}(S)$ belongs to the boundary that separates the two basins, as well as its preimages of any rank:

$$W^s(S) = \bigcup_{k\geq 0} T^{-k}\left(W^s_{loc}(S)\right) = \partial\mathcal{B}(E_1) \cap \partial\mathcal{B}(E_2) \tag{4.12}$$

Also in this case, in order to study the shape of $W^s(S)$, and the global bifurcations which change its structure, we first consider the symmetric case of homogeneous players. In this case, because of the symmetry of the map (4.2), the local stable set of S belongs to the invariant diagonal Δ. Indeed, as far as $\lambda(\mu+1) < 1$ the whole stable set belongs to Δ and is given by $W^s(S) = OO^{(1)}_{-1}$, where $O^{(1)}_{-1}$ is given in (4.9) and $OO^{(1)}_{-1}$ is the segment joining O with $O^{(1)}_{-1}$. In fact, as argued above, if $\lambda(\mu+1) < 1$ then the cusp point K of the critical curve $LC^{(b)}$ has negative coordinates and, consequently, the whole segment $OO^{(1)}_{-1}$ belongs to the region Z_2. This implies that the two preimages of any point of $OO^{(1)}_{-1}$ belong to Δ, and can be computed by the restriction (4.8). This proves that the segment $OO^{(1)}_{-1}$ is backward invariant, i.e., $T\left(OO^{(1)}_{-1}\right) = OO^{(1)}_{-1}$. In this case, the structure of the basins $\mathcal{B}(E_i)$, $i = 1, 2$, is very simple: $\mathcal{B}(E_1)$ is the portion of $\mathcal{B}$ below the diagonal Δ and $\mathcal{B}(E_2)$ is the portion of $\mathcal{B}$ above it. This situation is shown in Figure 10a. The line Δ of equal quantities is the only boundary between the two basins, hence any bounded trajectory starting with $q_1(0) > q_2(0)$ converges to the Nash equilibrium E_1 and any bounded trajectory starting with $q_1(0) < q_2(0)$ converges to the Nash equilibrium E_2. In economic terms this means that an initial difference in the quantities uniquely determines which of the equilibria is selected in the long run. If player 1 offers a larger quantity than player 2, then E_1 is selected, and vice-versa. Moreover, if $q_1(0) > q_2(0)$ $(q_1(0) < q_2(0))$ then $q_1(t) > q_2(t)$ $(q_1(t) < q_2(t))$ for any t, i.e. any initial order of the quantities of the two players is maintained during the whole time evolution of the duopoly game. In particular, both of the basins $\mathcal{B}(E_1)$ and $\mathcal{B}(E_2)$ are simply connected sets[8].

Their structure becomes much more complex for $\lambda(\mu+1) > 1$. This is shown in Figure 10b, obtained with $\mu = 3.4$ as in Figure10a, but $\lambda = 0.5 > 1/(\mu+1)$. In order to understand the bifurcation occurring at $\lambda(\mu+1) = 1$, we consider the critical curves of the map (4.2). In fact, at $\lambda(\mu+1) = 1$ a contact between $LC^{(b)}$ and the fixed point O occurs, due to the merging between O and the cusp point K. For $\lambda(\mu+1) > 1$ the portion KO of the segment $OO^{(1)}_{-1}$ belongs to the region Z_4 where four inverses of T exist. This implies that besides the two *rank-1* preimages on Δ the points of KO

[8] If condition $\lambda(\mu+1) < 1$ holds, this simple structure of the basins is conserved even if E_i are no longer stable and more complex bounded attractors exist around them.

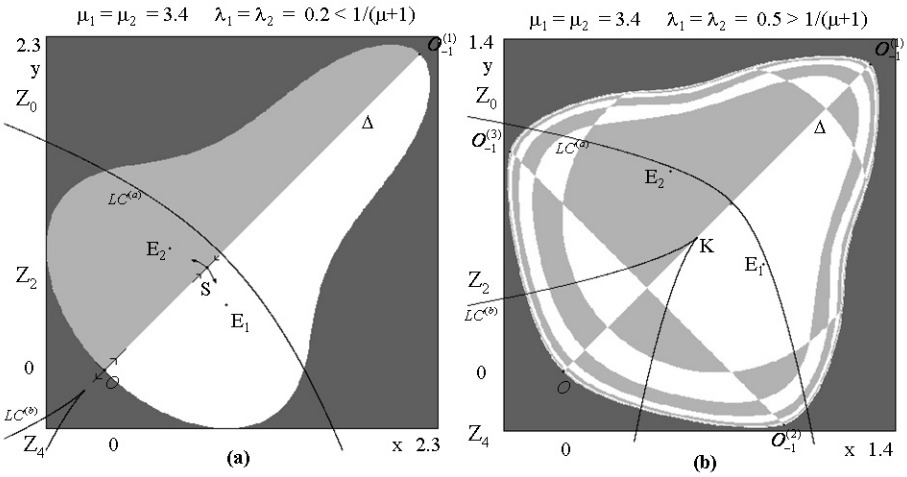

Figure 10.

have two further preimages located on the segment $O_{-1}^{(2)}O_{-1}^{(3)}$ of the line Δ_{-1}. Since $OO_{-1}^{(1)} = W_{loc}^{s}(S) \subset \partial\mathcal{B}(E_1) \cap \partial\mathcal{B}(E_2)$, also all the preimages of this segment belong to the boundary which separates $\mathcal{B}(E_1)$ from $\mathcal{B}(E_2)$. Furthermore, also the segment $O_{-1}^{(2)}O_{-1}^{(3)}$ has *rank-1* preimages, because portions of it are included in the regions Z_2 and Z_4. These are preimages of *rank-2* of $OO_{-1}^{(1)}$ and, consequently, belong to $W^s(S)$ according to (4.12). This repeated procedure, based on the iteration of the multivalued inverse of T, leads to the construction of the stable set $W^s(S)$ which is formed by the union of infinitely many arcs which accumulate on the boundary $\partial\mathcal{B}$. In fact the invariant set $\partial\mathcal{B}$, being a repelling set for the forward iteration of T, behaves as an attracting set for the iteration of the inverses of T.

The results given above can be summarized by the following proposition:

Proposition. *If $\mu_1 = \mu_2 = \mu$ and $\lambda_1 = \lambda_2 = \lambda$, the common boundary $\partial\mathcal{B}(E_1) \cap \partial\mathcal{B}(E_2)$ which separates the basin $\mathcal{B}(E_1)$ from the basin $\mathcal{B}(E_2)$ is given by the stable set $W^s(S)$ of the saddle point S. If $\lambda(\mu+1) < 1$ then $W^s(S) = OO_{-1}^{(1)}$, where $O = (0,0)$ and $O_{-1}^{(1)}$ is given by (4.9), and the two basins are simply connected sets; if $\lambda(\mu+1) > 1$ then the two basins are nonconnected sets, formed by infinitely many simply connected components.*

We would like to emphasize that the bifurcation occurring at $\lambda(\mu+1) = 1$ is a global bifurcation, i.e. it cannot be revealed by a study of the linear approximation of the dynamical system. The occurrence of such a bifurcation has been characterized by a contact between the stable set of S and a critical curve, and for this reason has been called *contact* bifurcation in Mira et al., 1996.

The occurrence of the bifurcation which transforms the basins from simply con-

nected to nonconnected causes a loss of predictability about the long-run evolution of our Cournot game starting from given initial quantities of the two players. In fact, if the initial quantities are sufficiently far away from a Nash equilibrium, for example near the boundary $\partial\mathcal{B}$ of $\mathcal{B}$, then the presence of the infinitely many components of both basins causes a sort of sensitivity with respect to these initial conditions. Even a very small perturbation of the initial condition of the Cournot game may lead to a crossing of the boundary which separates the two basins and, consequently, results in the convergence to a different Nash equilibrium.

We now move to the case of heterogeneous players, characterized by $\lambda_1 \neq \lambda_2$. In this case the local stable set $W^s_{loc}(S)$ is not along the diagonal Δ, because T is no longer symmetric and, consequently, Δ is no longer invariant. However, by numerical investigations, guided by the knowledge of the critical curves, we can analyze the structure of the basins of the two coexisting stable Nash equilibria and we can characterize the bifurcations that cause their qualitative changes.

In order to understand how complex basin structures are obtained, we start from a situation in which $W^s(S)$ has a simple shape, like the one shown in Figure 11a, obtained with $\mu = 3.6$, $\lambda_1 = 0.55$ and $\lambda_2 = 0.7$. The introduction of an asymmetry in the adaptive behavior of the players has a negligible effect on the local stability properties, since the eigenvalues of the two fixed points are exactly the same and are very close to the ones obtained in the homogeneous case with the same value for μ and with $\lambda = (\lambda_1 + \lambda_2)/2$. On the other hand, it causes an evident asymmetry of the basins of attraction. As shown in Figure 11a, when $\lambda_2 > \lambda_1$ the extension of $\mathcal{B}(E_2)$ is in general greater than the extension of $\mathcal{B}(E_1)$, and the complementary situation is obtained if λ_1 and λ_2 are swapped. Furthermore, even in situations characterized by a simple structure of the basins' boundaries, like the one shown in Figure 11a where both basins are connected sets, the statement that the initial order of the quantities is maintained along the whole trajectory is no longer true. In fact, in the case of different speeds of adjustment, say $\lambda_i > \lambda_j$, the typical occurrence is that the smaller basin $\mathcal{B}(E_j)$ is surrounded by points of $\mathcal{B}(E_i)$. Hence, the adjustment dynamic in our Cournot game may lead to convergence to E_i in the long run, even if players start with quantities which are closer to E_j.

In the situation shown in Figure 11a, the smaller basin $\mathcal{B}(E_1)$ is a simply connected set. The basin $\mathcal{B}(E_2)$ is a multiply connected set, due to the presence of a big "hole" (or "island", following Mira et al., 1994) nested inside it, whose points belong to $\mathcal{B}(E_1)$. Furthermore, $W^s(S)$, i.e. the boundary which separates the two basins, is entirely included inside the regions Z_2 and Z_0. However, the fact that in Figure 11a a portion of $W^s(S)$ is close to LC suggests the occurrence of a global bifurcation. In fact, if the parameters are changed, so that a contact between $W^s(S)$ and LC occurs, this contact marks a bifurcation which causes qualitative changes in the structure of the basins. If a portion of $\mathcal{B}(E_1)$ enters Z_4 after a contact with $LC^{(b)}$, new *rank-1* preimages of that portion will appear near $LC^{(b)}_{-1}$, and such preimages must belong to $\mathcal{B}(E_1)$. Indeed, this is the situation shown in Figure11b, obtained after a small change of λ_1. The portion of $\mathcal{B}(E_1)$ inside Z_4 is denoted by H_0. It has two *rank-1* preimages, denoted by $H^{(1)}_{-1}$ and $H^{(2)}_{-1}$, which are located at opposite sides with respect to $LC^{(b)}_{-1}$ and merge on it (in fact, by definition, the *rank-1* preimages of the arc of $LC^{(b)}$ which bound H_0 must merge

along $LC_{-1}^{(b)}$). The set $H_{-1} = H_{-1}^{(1)} \cup H_{-1}^{(2)}$ constitutes a nonconnected portion of $\mathcal{B}(E_1)$. Moreover, since H_{-1} belongs to the region Z_4, it has four *rank-1* preimages, denoted by $H_{-2}^{(j)}$, $j = 1, ..., 4$, which constitute other four "islands" of $\mathcal{B}(E_1)$, or "holes" of $\mathcal{B}(E_2)$. Points of these "islands" are mapped into H_0 in two iterations of the map T. Indeed, infinitely many higher rank preimages of H_0 exist, thus giving infinitely many smaller and smaller disjoint "islands" of $\mathcal{B}(E_1)$. Hence, at the contact between $W^s(S) = \partial\mathcal{B}(E_1)$ and LC the basin $\mathcal{B}(E_1)$ is transformed from a simply connected into a nonconnected set, constituted by infinitely many disjoint components. The larger connected component of $\mathcal{B}(E_1)$ which contains E_1 is the *immediate basin* $\mathcal{B}_0(E_1)$, and the whole basin is given by the union of the infinitely many preimages of $\mathcal{B}_0(E_1)$.

Such contact bifurcations can only be revealed numerically, since the equations of the curves involved in the contact cannot be analytically expressed in terms of elementary functions. This happens frequently in nonlinear dynamical systems of dimension greater than one, where the study of global bifurcations is generally obtained through an interplay between theoretical and numerical methods, and the occurrence of these bifurcations is shown by computer-assisted proofs, based on the knowledge of the properties of the critical curves and their graphical representation (see e.g. Mira et al., 1996, for many examples). This "modus operandi" is typical in the study of the global bifurcations of nonlinear two-dimensional maps.

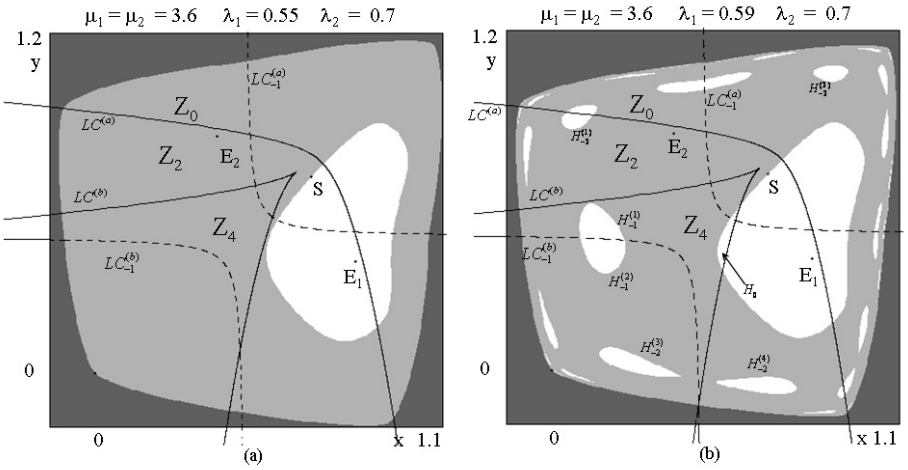

Figure 11.

An extension of such methods to the study of higher dimensional noninvertible maps is not easy in general. Indeed, some non-trivial practical problems arise, related to the obvious reason that the computer screen is two-dimensional, so the visualization of objects in a phase spaces of dimension greater than two, and the detection of contacts among these objects as their shapes change, may become a very difficult task. For

example, in Agiza et al., 1999, a repeated Cournot game is considered, whose time evolution is obtained by the iteration of the three-dimensional map $T : (q_1, q_2, q_3) \rightarrow (q_1', q_2', q_3')$

$$T : \begin{cases} q_1' = (1-\lambda_1)\, q_1 + \lambda_1 \mu_1 \left[q_2 \left(1 - q_2\right) + q_3 \left(1 - q_3\right) \right] \\ q_2' = (1-\lambda_2)\, q_2 + \lambda_2 \mu_2 \left[q_3 \left(1 - q_3\right) + q_1 \left(1 - q_1\right) \right] \\ q_3' = (1-\lambda_3)\, q_3 + \lambda_3 \mu_3 \left[q_1 \left(1 - q_1\right) + q_2 \left(1 - q_2\right) \right] \end{cases} \tag{4.13}$$

which can be seen as the extension of the game illustrated above to the case of three players. In Agiza et al., 1999, two-dimensional sections are employed in order to visualize the basins of coexisting attractors, but this method is not useful to detect the contact bifurcations which cause changes in the structure of the basins. The same game has been re-examined in Bischi et al., 2001, where enhanced graphical methods have been used to modulate the opacity of the outer objects in order to visualize objects which are nested inside them. Moreover, the critical sets, which are now two-dimensional surfaces embedded in a three-dimensional phase space, have been represented like semi-transparent veils, so that their contacts with portions of basin boundaries, also given by two-dimensional surfaces, can be detected.

4.2 A duopoly game with gradient dynamics

In this section we consider a Cournot duopoly game, proposed by Bischi and Lamantia, 2002a, where two firms produce quantities q_1 and q_2 in a market characterized by a linear demand function $p = a - b(q_1 + q_2)$ with nonlinear cost functions $C_i = c_i q_i/(1 + \gamma_{ij} q_j)$ $i = 1, 2,\ j \neq i$. At discrete time periods each player decides, given the competitor's action, its own production in order to maximize the expected profit

$$\pi_i(q_1, q_2) = q_i \left[a - b \left(q_1 + q_2 \right) \right] - \frac{c_i q_i}{1 + \gamma_{ij} q_j} \ ;\ i, j = 1, 2,\ i \neq j \tag{4.14}$$

From the first order conditions $\partial \pi_i / \partial q_i = 0$, we can easily get the reaction functions[9]

$$q_i = r_i(q_j) = \frac{1}{2b} \left(a - b q_j - \frac{c_i}{1 + \gamma_{ij} q_j} \right). \tag{4.15}$$

For a given expected production of the competitor, r_i represents the "Best Reply" of the quantity-setting firm i according to its optimization problem. In Bischi and Lamantia, 2002a, it is proved that these two reaction functions have a unique positive intersection, say E_*, that represents the unique Nash equilibrium of the game.

Although fully rational players are assumed to reach the Nash equilibrium immediately (in one shot), an important issue in economic literature concerns the outcome of the game when agents are not fully rational. In Bischi and Lamantia, 2002a, a repeated Cournot duopoly game is proposed where two boundedly rational players update their production strategies at discrete time periods by an adjustment mechanism based on a local estimate of the marginal profit $\partial \pi_i / \partial q_i$: At each time period t a firm decides to increase (decrease) its production for period $t + 1$ if it perceives positive (negative)

[9] A simple check of the second derivatives testifies that these solutions indeed represent local profit maxima, provided that the quantities are non negative.

marginal profit on the basis of information held at time t, according to the following dynamic adjustment mechanism (see e.g. Bischi and Naimzada, 2000)

$$q_i(t+1) = q_i(t) + \alpha_i(q_i(t))\frac{\partial \pi_i}{\partial q_i}\left(q_1(t), q_2(t)\right) \quad ; \qquad i = 1, 2 \tag{4.16}$$

where $\alpha_i(q_i)$ is a positive function which gives the extent of production variation of *ith* firm following a given profit signal. A Nash equilibrium, defined by the first order conditions $\partial \pi_i / \partial q_i = 0$, is a stationary point of the dynamical system. We assume linear functions $\alpha_i\left(q_i\right) = v_i q_i$, $i = 1, 2$, since this assumption captures the fact that *relative* production variations are proportional to marginal profits, i.e. $\frac{q_i(t+1)-q_i(t)}{q_i(t)} = v_i \frac{\partial \pi_i}{\partial q_i}$, where v_i is a positive *speed of adjustment*. With these assumptions, together with the profit functions given in (4.14), we obtain a discrete dynamical system of the form $(q_1(t+1), q_2(t+1)) = T\left(q_1(t), q_2(t)\right)$, with the map $T : \mathbb{R}^2 \to \mathbb{R}^2$ given by

$$T : \begin{cases} q_1' = q_1 + v_1 q_1 \left[a - 2bq_1 - bq_2 - \frac{c_1}{1+\gamma_{12} q_2}\right] \\ q_2' = q_2 + v_2 q_2 \left[a - 2bq_2 - bq_1 - \frac{c_2}{1+\gamma_{21} q_1}\right] \end{cases} \tag{4.17}$$

Besides the equilibrium point E_*, located at the intersections of the reaction curves (4.15), the map (4.17) has three boundary equilibria located along the coordinate axes:

$$E_0 = (0, 0), \quad E_1 = (\frac{a - c_1}{2b}, 0), \quad E_2 = (0, \frac{a - c_2}{2b}). \tag{4.18}$$

The fixed points E_1 and E_2 can be denoted as *monopoly equilibria* provided that $c_i < a$, $i = 1, 2$. It is worth to note that the coordinate axes $q_i = 0$, $i = 1, 2$, are invariant submanifold, i.e. if $q_i = 0$ then $q_i^{'} = 0$. This means that starting from an initial condition on a coordinate axis (*monopoly case*) the dynamics are trapped into the same axis for each t, thus giving *monopoly dynamics*, governed by the restriction of the map T to that axis. Such a restriction is given by the following one-dimensional map, obtained from (4.17) with $q_i = 0$

$$q_j = (1 + v_j(a - c_j))q_j - 2bv_j q_j^2 \qquad\qquad j \neq i \ . \tag{4.19}$$

This map is conjugate[10] to the standard logistic map (2.7) through the linear transformation

$$q_j = \frac{1 + v_j(a - c_j)}{2bv_j} x \tag{4.20}$$

from which we obtain the relation $\mu = 1 + v_j(a - c_j)$.

If $\gamma_{12} = \gamma_{21} = 0$ the map (4.17) reduces to the one studied in Bischi and Naimzada, 2000, where it is shown that unbounded trajectories are obtained if the initial condition is taken sufficiently far from the Nash equilibrium[11], hence E_* cannot be globally stable.

[10] See Devaney, 1987.

[11] From an economic point of view, diverging trajectories do not represent interesting evolutions, as they can be interpreted as an irreversible departure from optimality.

As in the previous model, we denote by $\mathcal{B}$ the set of points which generate feasible trajectories and by $\mathcal{B}(\infty)$ the set of initial conditions whose trajectories diverge. A feasible trajectory may converge to the Nash equilibrium E_*, to another more complex attractor inside $\mathcal{B}$ or to a one-dimensional invariant set embedded inside a coordinate axis, when one competitor exits the market. However, when the Nash equilibrium exists the coordinate axes are transversely unstable, so they behave as repelling sets with respect to trajectories approaching them from the interior of the nonnegative orthant, and consequently evolutions of the duopoly game toward monopoly situations are excluded.

Let us first consider the dynamics of T restricted to the invariant axis $q_2 = 0$. From the one-dimensional restriction defined in (4.19), we can deduce that bounded trajectories along that invariant axis are obtained for $v_1(a - c_1) \leq 3$ (corresponding to $\mu \leq 4$ in (4.20)), provided that the initial conditions are taken inside the segment $\omega_1 = OO_{-1}^{(1)}$, where $O_{-1}^{(1)}$ is the *rank-1* preimage of the origin O computed according to the restriction (4.19), i.e.

$$O_{-1}^{(1)} = \left(\frac{v_1(a - c_1)}{2bv_1}, 0 \right) \tag{4.21}$$

and divergent trajectories along the invariant q_1 axis are obtained starting from an initial condition out of the segment ω_1. Analogously, when $v_2(a-c_2) \leq 3$, bounded trajectories along the invariant q_2 axis are obtained provided that the initial conditions are taken inside the segment $\omega_2 = OO_{-1}^{(2)}$, where

$$O_{-1}^{(2)} = \left(0, \frac{v_2(a - c_2)}{2bv_2} \right). \tag{4.22}$$

and, also in this case, divergent trajectories along the q_2 axis are obtained starting from an initial condition out of the segment ω_2.

Consider now the region bounded by the segments ω_1 and ω_2 and their *rank-1* preimages, say ω_1^{-1} and ω_2^{-1} respectively. Such preimages can be analytically computed as follows. Let $X = (x, 0)$ be a point of ω_1. Its preimages are the real solutions (q_1, q_2) of the algebraic system obtained from (4.17) with $(q_1', q_2') = (x, 0)$:

$$\begin{cases} q_1 \left[1 + v_1 \left(a - 2bq_1 - bq_2 - \frac{c_1}{1+\gamma_{12} q_2} \right) \right] = x \\ q_2 \left[1 + v_2 \left(a - 2bq_2 - bq_1 - \frac{c_2}{1+\gamma_{21} q_1} \right) \right] = 0 \,. \end{cases} \tag{4.23}$$

It is an easy exercise to show that the preimages of the points of ω_1 are either located on the same invariant axis $q_2 = 0$ or on the curve of equation

$$q_2 = r_2(q_1) + \frac{1}{2bv_2}. \tag{4.24}$$

where r_2 is the reaction function defined in (4.15). Analogously, the preimages of a point $Y = (0, y)$ of ω_2 belong to the same invariant axis $q_1 = 0$ or to the curve of equation

$$q_1 = r_1(q_2) + \frac{1}{2bv_1}. \tag{4.25}$$

where r_1 is the reaction function defined in (4.15). The curve (4.24) intersects the q_2 axis in the point $O_{-1}^{(2)}$ and the curve (4.25) intersects the q_1 axis in the point $O_{-1}^{(1)}$. Moreover, the two curves intersect at a point $O_{-1}^{(3)}$, which is another *rank-1* preimage of $O = (0, 0)$. These four *rank-1* preimages of the origin are the vertexes of a "quadrilateral" $OO_{-1}^{(1)}O_{-1}^{(3)}O_{-1}^{(2)}$, whose sides are ω_1, ω_2 and their *rank-1* preimages located on the curves of equation (4.24) and (4.25) respectively, denoted by ω_1^{-1} and ω_2^{-1} in Figures 12a, b. It is evident that the sides $O_{-1}^{(2)}O_{-1}^{(3)}$ and $O_{-1}^{(3)}O_{-1}^{(1)}$, given by ω_1^{-1} and ω_2^{-1} of equation (4.24) and (4.25) respectively, are parallel translations of the reaction curves R_2 and R_1, shifted of $\frac{1}{2bv_i}$, $i = 2, 1$, respectively. All the points outside this quadrilateral cannot generate feasible trajectories. In fact, the points located on the right of ω_2^{-1} are mapped into points with negative q_1 after one iteration, as can be easily deduced from the first component of (4.17), and the points located above ω_1^{-1} are mapped into points with negative q_2 after one iteration, as can be deduced from the second component of (4.17).

For $\gamma_{12} = \gamma_{21} = 0$ the curves ω_1^{-1} and ω_2^{-1} reduce to straight lines, as already proved in Bischi and Naimzada, 2000. This situation is shown in Figure12a, obtained with $v_1 = 0.2$, $v_2 = 0.25$, $c_1 = 3$, $c_2 = 4$ and $\gamma_{12} = \gamma_{21} = 0$. With this set of parameters the Nash equilibrium E_* is stable, and the set $\mathcal{B}$ coincides with the basin of E_*. As it can be seen in Figure 12a, where the numerically computed basin of E_* is represented by the white region and the basin of infinity by the grey one, the boundary $\partial\mathcal{B}$ is formed by ω_1, ω_2 and their *rank-1* preimages ω_1^{-1} and ω_2^{-1} of equations (4.24) and (4.25) respectively, which are parallel to the reaction curves R_2 and R_1 (shown in Figure 12). In Figure 12b one of the spillover parameters is positive, namely $\gamma_{21} = 3$, and the other parameters are the same as in Figure 12a. It can be noticed that in this case the upper boundary, belonging to the curve ω_1^{-1}, is concave.

The simple shape of $\partial\mathcal{B}$ shown in Figure 12 is due to the fact that only preimages of *rank-1* of ω_i exist. In fact, ω_1^{-1} and ω_2^{-1} are entirely included inside a region of the plane whose points have no preimages. The situation is different when the values of the parameters are such that some portions of these curves belong to regions whose points have preimages, which constitute preimages of rank higher than one of the segments ω_i. In this case the set $\mathcal{B}$ has a more complex topological structure. Also in this case, the transitions between qualitatively different structures of the basins can be described in terms of contacts between $\partial\mathcal{B}$ and arcs of *critical curves*. In fact, the map defined in (4.17) is noninvertible, since given a point $(q_1', q_2') \in \mathbb{R}^2$ its preimages, computed by solving the sixth degree algebraic system (4.17), may be up to six. For instance, as shown above, the origin $O = (0, 0)$ can have four *rank-1* preimages, given by O itself and $O_{-1}^{(i)}$, $i = 1, 2, 3$.

For a given set of parameters, the critical curves of the map (4.17) can be easily obtained numerically. For example, for the set of parameters used to obtain Figure 13a, i.e. $v_1 = 0.25$, $v_2 = 0.3$, $c_1 = 4$, $c_2 = 3$ and $\gamma_{12} = 2$, $\gamma_{21} = 4$, the numerically computed set of points at which the Jacobian vanishes is formed by the union of two branches, denoted by $LC_{-1}^{(a)}$ and $LC_{-1}^{(b)}$ in Figure 13a., where $LC^{(b)}$ separates the region Z_0, whose points have no preimages, from the region Z_2, whose points have two distinct *rank-1*

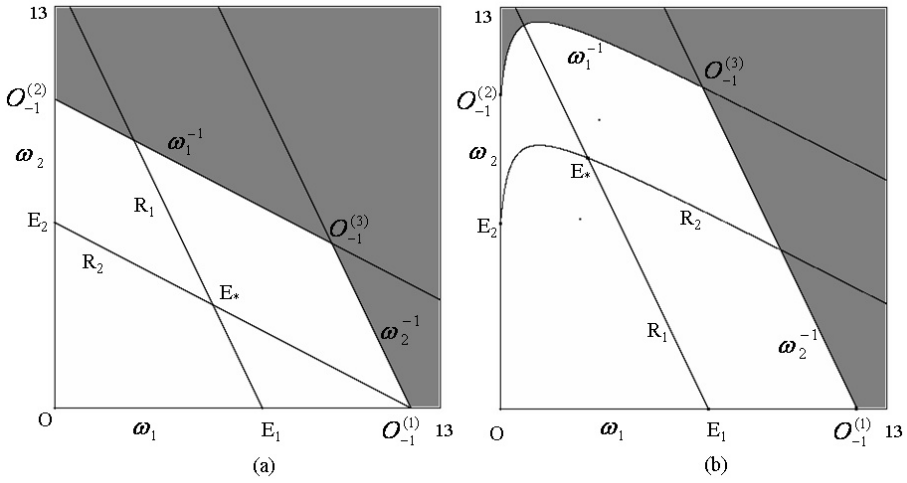

Figure 12.

preimages, and $LC^{(a)}$ separates the region Z_2 from Z_4, whose points have four distinct preimages.

The curve $LC_{-1}^{(b)}$ intersects the q_i axis at the point of maximum of the restriction (4.19), given by $M_{-1}^i = \frac{1+v_i(a-c_i)}{4bv_i}$, and the curve $LC^{(b)}$ intersects the q_i axis at the corresponding maximum value $M^i = \frac{[1+v_i(a-c_i)]^2}{8bv_i}$ of the restriction (4.19).

In Figure 13a $\mathcal{B}$ is a simply connected set, with the boundary $\partial\mathcal{B}$ having the "quadrilateral shape" described above, because the preimages ω_i^{-1}, $i = 1, 2$, of the invariant axes, are entirely included inside the region Z_0, so that no preimages of higher rank exist. The situation would be different if some portions of these lines were inside the regions Z_2 or Z_4. Indeed, the fact that a portion of $LC^{(b)}$ is close to $\partial\mathcal{B}$ suggests that a contact bifurcation may occur if some parameter is varied. In fact, if a portion of $\mathcal{B}(\infty)$ enters Z_2 after a contact of $\partial\mathcal{B}$ with $LC^{(b)}$, then new preimages of that portion will appear near $LC_{-1}^{(b)}$ and such preimages must belong to $\mathcal{B}(\infty)$. This is the situation illustrated by Figure 13b, obtained after an increase of the spillover parameters, i.e. $\gamma_{12} = 3$ and $\gamma_{21} = 7$. In fact, after a contact between $\partial\mathcal{B}$ and $LC^{(b)}$, a portion of $\mathcal{B}(\infty)$, say H_0 (bounded by a portion of ω_1^{-1} and LC) which was in region Z_0 before the bifurcation, enters inside Z_2. The points belonging to H_0 have two distinct preimages, located at opposite sides with respect to the line LC_{-1}, with the exception of the points of the curve $LC^{(b)}$ inside $B(\infty)$ whose preimages, according to the definition of LC, merge on $LC_{-1}^{(b)}$. Since H_0 is part of $\mathcal{B}(\infty)$ also its preimages belong to $\mathcal{B}(\infty)$. In other words, the *rank-1* preimages of H_0 are formed by two areas joining along LC_{-1} and constitutes a *hole* of $\mathcal{B}(\infty)$ nested inside $\mathcal{B}$. This is the largest hole appearing in Figure 13b, and is called the *main hole*. It lies inside region Z_2, hence it has 2 preimages, which are smaller holes bounded by preimages of rank 3 of ω_1. Even these are both inside Z_2, so each of

them has two further preimages inside Z_2, and so on. Now the boundary $\partial\mathcal{B}$ is formed by the union of an external part, given by the coordinate axes and their *rank-1* preimages (4.24) and (4.25), and the boundaries of the holes, which are sets of preimages of higher rank of ω_1. So, the global bifurcation just described transforms a *simply connected* basin into a *multiply connected* one, with a countable infinity of holes inside, called *arborescent sequence of holes* (see Mira et al., 1994, Mira et al., 1996, Abraham et al., 1997).

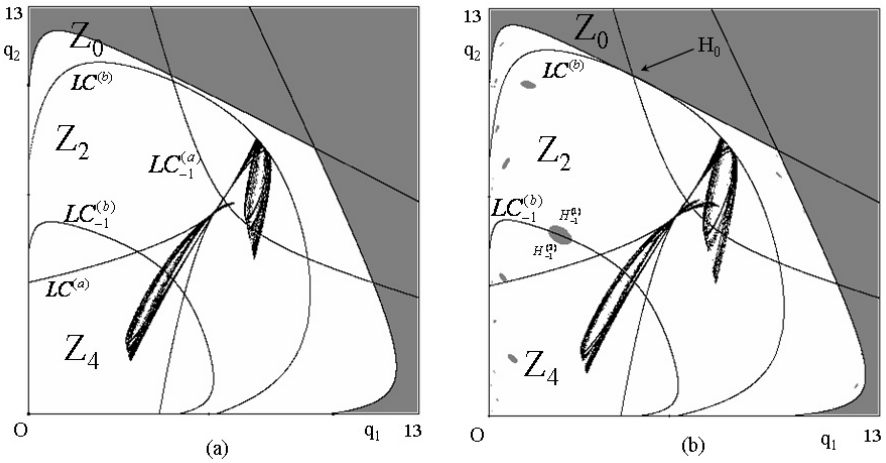

Figure 13.

5 Symmetric dynamical systems, Milnor attractors and riddled basins

In this section we consider an extension of the notion of attractor, known as *Milnor attractor* (after Milnor, 1985), whose basin of attraction may assume a structure, called *riddled basin*, characterized by an extreme form of complexity, according to the following definitions (see Alexander et al., 1992, Ashwin et al., 1996, Buescu, 1997). The more general notion of Milnor attractor has been introduced to evidence the existence of invariant sets which "attract" many points even if they are not attractors in the usual topological sense.

A closed invariant set $\mathcal{A}$ is said to be a *weak attractor in Milnor sense* (or simply *Milnor attractor*) if its stable set $\mathcal{B}(\mathcal{A})$, i.e. the set of points whose ω-limit sets of x belongs to $\mathcal{A}$[12],has positive Lebesgue measure.

If $\mathcal{A}$ is a Milnor attractor, then its stable set $\mathcal{B}(A)$ is called "riddled basin" if it is such that any neighborhood of it contains points whose trajectory converge to another attrac-

[12]The $\omega-$limit set of x is the set of accumulation points of $T^t(x)$, as $t \to \infty$.

tor. In other words, a riddled basin does not include any open subset, so it corresponds to an extreme form of uncertainty.

This section is mainly devoted to riddled basins, as well as to the global bifurcations leading to their creation.

Note that an attractor in the usual (topological) sense is also a Milnor attractor, but the converse is not true. In fact, a topological attractor is such that its basin $\mathcal{B}(\mathcal{A})$ contains an open neighborhood of $\mathcal{A}$, whereas for a Milnor attractor initial conditions arbitrarily close to $\mathcal{A}$ can generate trajectories that are locally repelled out from $\mathcal{A}$. In this case $\mathcal{B}(\mathcal{A})$ is called "realm of attraction" (Milnor, 1985) reserving the term "basin" when $\mathcal{B}(\mathcal{A})$ is an open set. However, since the term basin is more standard in the literature, we shall use such term even when $\mathcal{A}$ is a Milnor (but not topological) attractor, for which $\mathcal{B}(\mathcal{A})$ is not, in general, an open set.

Restricting an n-dimensional dynamical system with phase space S to an invariant lower dimensional submanifold $N \subset S$, (i.e. $T(N) \subseteq N$), the map $g = T|_N : N \to N$ determines a discrete dynamical system in its own. The trajectories embedded into N, whose dynamics are governed by the lower dimensional restriction g, are called *synchronized trajectories*. The existence of such lower dimensional dynamics embedded into the n-dimensional phase space of T rises the question, recently investigated by many authors, if an attractor A_N of g in N is also an attractor of the map T, and in which sense (see e.g. Buescu, 1997, and references therein). Of course, an attractor A_N of the restriction g is stable with respect to perturbations on N, so an answer to this question can be given through a study of the stability of A_N with respect to perturbations transverse to N (*transverse stability*). Results on transverse stability have mainly been studied when the dynamics restricted to the invariant submanifold are chaotic. In this case the question of transverse stability is related to the phenomenon of *chaos synchronization* (i.e. when trajectories starting out of N are attracted toward a chaotic attractor $A_N \subseteq N$).

These phenomena have recently raised interest in many fields, ranging from electrical engineering and communication systems to ecology and chemistry (see e.g. Fujisaka and Yamada, 1983, Ferretti, 1988, Pecora and Carrol, 1990, Ashwin et al., 1996, Buescu, 1997). Applications in economic modelling have recently been proposed in Bischi et al., 1999a, Bischi and Gardini, 1998, 2000, Kopel et al., 2000, Bischi and Lamantia, 2002b.

The particular feature of the invariance of a submanifold of lower dimension is a standard occurrence if the map T has some symmetry property, a situation that often occurs in applications. Measure theoretic, but not stable in Lyapunov sense, attractors appear quite naturally in this context, together with new and striking phenomena, like on-off intermittency and riddled basins, and also new kinds of bifurcations, like riddling (or bubbling) bifurcations and blowout bifurcations.

Maps with symmetry properties arise quite naturally in dynamical models of competition. In fact, when two competitors behave identically, the state variables that represent the competitors' choices can be swapped without changing the dynamical system. This means that the system has a symmetry property and, consequently, an invariant submanifold.

Let us consider, for example, the case of two competitors that choose their actions, measured by $x_1(t)$ and $x_2(t)$ respectively, at discrete time periods, and assume that this process is modelled by the iterations of a two-dimensional map $T : S \to S$, $S \subseteq \mathbb{R}^2$. In

the case of identical competitors, the map T must remain the same under the exchange of the players, i.e. $T \circ P = P \circ T$, where $P : (x_1, x_2) \to (x_2, x_1)$ denotes the reflection through the diagonal $\Delta = \left\{(x_1, x_2) \in \mathbb{R}^2 | x_1 = x_2\right\}$. This symmetry property implies that the diagonal is mapped into itself by T, i.e. $T(\Delta) \subseteq \Delta$.

In this case, the *synchronized trajectories* are embedded into Δ, i.e. are characterized by identical choices $x_1(t) = x_2(t)$ for every t. This invariance property translates the obvious statement that identical players, starting with identical initial strategies $x_1(0) = x_2(0)$, behave identically for each $t \geq 0$, even if each of them behaves chaotically, and the common behavior of the two players is summarized by the dynamics of the simpler one-dimensional map $g = T|_\Delta : \Delta \to \Delta$.

An important question is whether trajectories starting with initial condition outside of Δ, i.e. when $x_1(0) \neq x_2(0)$, will evolve toward synchronization, i.e. $|x_1(t) - x_2(t)| \to 0$ as $t \to +\infty$, so that the long-run behavior is governed by the one-dimensional attractors of the restriction g. Of course, the attracting sets of the map g are stable with respect to perturbations along Δ, hence an answer to the question addressed above requires a local study of the stability with respect to perturbations transverse to Δ (*transverse stability*). When the attractors of g embedded inside Δ are chaotic, they may be Milnor (but not topological) attractors of the two-dimensional dynamical system, and their basins may be riddled.

In Bischi et al., 1999a, Kopel et al., 2000, the one-dimensional restriction $g : \Delta \to \Delta$ has been considered as the model of a *representative agent* whose dynamics summarize the common behavior of the two synchronized competitors, so the study of the asymptotic synchronization has been related to the common assumption, often made in economic modeling, that the behavior of a system with many identical agents can be summarized by that of a "representative agent", a point that has been recently criticized by some authors (see Kirman, 1992, Aoki, 1996).

5.1 Some basic definitions and results

Let A_Δ be a chaotic attractor (with absolutely continuous invariant measure on it) of g, the restriction to Δ of the bidimensional map T. The key property for the study of the transverse stability of A_Δ is that it includes infinitely many periodic orbits which are unstable in the direction along Δ. For any of these cycles it is easy to compute the associated eigenvalues. In fact, due to the symmetry of the map, the Jacobian matrix of T, computed at any point of Δ, say $DT(x, x) = \{T_{ij}(x)\}$, is such that $T_{11} = T_{22}$ and $T_{12} = T_{21}$. The two orthogonal eigenvectors of such a symmetric matrix are one parallel to Δ, say $\mathbf{v}_\parallel = (1, 1)$, and one perpendicular to it, say $\mathbf{v}_\perp = (1, -1)$, with related eigenvalues given by

$$\lambda_\parallel(x) = T_{11}(x) + T_{12}(x) \quad \text{and} \quad \lambda_\perp(x) = T_{11}(x) - T_{12}(x)$$

respectively. Of course, $\lambda_\parallel(x) = g'(x)$. Since the product of matrices with the structure of $DT(x, x)$ has the same structure as well, a k-cycle $\{x_1, ..., x_k\}$ embedded into Δ has eigenvalues $\lambda_\parallel^k = \prod_{i=1}^k \lambda_\parallel(x_i)$ and $\lambda_\perp^k = \prod_{i=1}^k \lambda_\perp(x_i)$, with eigenvectors $\mathbf{v}_\parallel$ and $\mathbf{v}_\perp$ respectively. So, for a chaotic set $A_\Delta \subset \Delta$, infinitely many transverse Lyapunov exponents

can be defined as

$$\Lambda_{\perp} = \lim_{N\to\infty} \frac{1}{N} \sum_{i=0}^{N} \ln |\lambda_{\perp}(x_i)| \tag{5.1}$$

where $\{x_i = g^i(x_0), i \geq 0\}$ is a trajectory embedded in A_{Δ}. If x_0 belongs to a k-cycle then $\Lambda_{\perp} = \ln |\lambda_{\perp}^k|$, so that the cycle is transversely stable if $\Lambda_{\perp} < 0$, whereas if x_0 belongs to a generic aperiodic trajectory embedded inside the chaotic set A_{Δ} then $\Lambda_{\perp}$ is the *natural transverse Lyapunov exponent* $\Lambda_{\perp}^{nat}$. By the term "natural" we mean the Lyapunov exponent associated to the natural, or SBR (Sinai-Bowen-Ruelle), measure, i.e., computed for a typical trajectory taken in the chaotic attractor A_{Δ}. Since infinitely many cycles, all unstable along Δ, are embedded inside a chaotic attractor A_{Δ}, a spectrum of transverse Lyapunov exponents can be defined (see Buescu, 1997)

$$\Lambda_{\perp}^{\min} \leq ... \leq \Lambda_{\perp}^{nat} \leq ... \leq \Lambda_{\perp}^{\max} \tag{5.2}$$

The meaning of the inequalities in (5.2) can be intuitively understood on the basis of the property that $\Lambda_{\perp}^{nat}$ expresses a sort of "weighted balance" between the transversely repelling and transversely attracting cycles (see Nagai and Lai, 1997). If $\Lambda_{\perp}^{\max} < 0$, i.e. all the cycles embedded in A_{Δ} are transversely stable, then A_{Δ} is asymptotically stable, in the usual Lyapunov sense, for the two-dimensional map T. However, it may occur that some cycles embedded in the chaotic set A_{Δ} become transversely unstable, i.e. $\Lambda_{\perp}^{\max} > 0$, while $\Lambda_{\perp}^{nat} < 0$. In this case, A_{Δ} is no longer Lyapunov stable, but it continues to be an attractor in the weaker Milnor sense. The transition from asymptotic stability to attractivity only in Milnor sense, marked by a change of sign of $\Lambda_{\perp}^{\max}$ from negative to positive, is denoted as *riddling bifurcation* in Lai and Grebogi, 1996 (or *bubbling bifurcation* in Venkataramani, 1996).

Even if the occurrence of such bifurcation is detected through the study of the transverse Lyapunov exponents, its effects depend on the action of the nonlinearities far from Δ, that is, on the global properties of the dynamical system. In fact, after the riddling bifurcation two possible scenarios can be observed, according to the fate of the trajectories that are locally repelled along (or near) the local unstable manifolds of the transversely repelling cycles:

(**L**) they can be reinjected towards Δ, so that the dynamics of such trajectories are characterized by some bursts far from Δ before synchronizing on it (a very long sequence of such bursts, which can be observed when $\Lambda_{\perp}$ is close to zero, has been called *on-off intermittency* in Ott and Sommerer, 1994);

(**G**) they may belong to the basin of another attractor, in which case the phenomenon of *riddled basins* is obtained (see Alexander et al., 1992).

Some authors call *local riddling* the situation (**L**) and, by contrast, *global riddling* the situation (**G**) (see Ashwin et al., 1996, Maistrenko et al., 1997). When also $\Lambda_{\perp}^{nat}$ becomes positive, due to the fact that the transversely unstable periodic orbits embedded into A_{Δ} have a greater weight as compared with the stable ones, a *blowout bifurcation* occurs, after which A_{Δ} is no longer a Milnor attractor, because it attracts a set of points of zero measure, and becomes a *chaotic saddle*. In particular, for $\lambda_{\perp}^{\min} > 0$ all the cycles embedded into Δ are transversely repelling, and A_{Δ} is called *normally repelling chaotic saddle*.

Also the macroscopic effect of a blowout bifurcation is strongly influenced by the behavior of the dynamical system far from the invariant submanifold Δ: trajectories starting close to the chaotic saddle may be attracted by some attracting set far from Δ or remain inside a two-dimensional compact set located around the chaotic saddle A_Δ, thus giving on-off intermittency.

So, the effects of these bifurcations are related to the action of the nonlinearities acting far from Δ. When T is a noninvertible map, as generally occurs in problems of chaos synchronization[13], the global dynamical properties can be usefully described by the method of *critical curves* and the reinjection of the locally repelled trajectories can be described in terms of their folding action. This idea has been recently proposed in Bischi and Gardini, 1998, Bischi and Gardini, 2000 for the study of symmetric maps arising in game theory, and in Bischi et al., 1999a, for the study of the effects of small asymmetries due to parameters mismatches, see also Bischi and Lamantia, 2002b, where the concept of *correlated chaos* is introduced. In these papers, the critical curves have been used to obtain the boundary of a compact trapping region, called *absorbing area* following Mira et al., 1996, inside which intermittency and blowout phenomena are confined. In particular, in Bischi and Gardini, 1998, the concept of *minimal invariant absorbing area* is defined in order to give a global characterization of the different dynamical scenarios related to riddling and blowout bifurcations.

Before giving an example, let us recall some properties of critical curves and absorbing areas (see Mira et al., 1996, chap. 4, or Bischi and Gardini, 1998, for more details).

The critical sets of rank k are defined as the images of rank k of LC_{-1} denoted by $LC_{k-1} = T^k(LC_{-1}) = T^{k-1}(LC)$, LC_0 being LC. Segments of critical curves of *rank-k*, $k = 0, 1, ...$, can be used in order to define trapping regions of the phase plane. An *absorbing area* $\mathcal{A}$ is a bounded region of the plane whose boundary is given by critical curve segments (segments of the critical curve LC and its images) such that a neighborhood $U \supset \mathcal{A}$ exists whose points enter $\mathcal{A}$ after a finite number of iterations and then never escape it, i.e. $T(\mathcal{A}) \subseteq \mathcal{A}$.

Following Mira et al., 1996 (see also Puu, 2000) a practical procedure can be outlined in order to obtain the boundary of an absorbing area (although it is difficult to give a general method). Starting from a portion of LC_{-1}, approximately taken in the region occupied by the area of interest, its images of increasing rank are computed until a closed region is obtained. When such a region is mapped into itself, then it is an absorbing area $\mathcal{A}$. The length of the initial segment is to be taken, in general, by a trial and error method, although several suggestions are given in the books referenced above. Once an absorbing area $\mathcal{A}$ is found, in order to see if it is invariant (or strictly mapped into itself) the same procedure must be repeated by taking only the portion $\gamma = \mathcal{A} \cap LC_{-1}$as the starting segment. Then one of the following two cases occurs:

(i) the union of m iterates of γ (for a suitable m) covers the whole boundary of $\mathcal{A}$; in

[13]In fact the one-dimensional restriction g must be a noninvertible map in order to have chaotic motion along the invariant subspace Δ.

which case $\mathcal{A}$ is an invariant absorbing area, and

$$\partial\mathcal{A} \subset \bigcup_{k=1}^{m} T^k(\gamma) \tag{5.3}$$

(ii) no natural m exists such that $\bigcup_{i=1}^{m} T^i(\gamma)$ covers the whole boundary of $\mathcal{A}$, in which case $\mathcal{A}$ is not invariant but strictly mapped into itself. An invariant absorbing area is obtained by $\cap_{n>0} T^n(\mathcal{A})$.

The *minimal invariant absorbing area* is the smallest absorbing area that includes the Milnor attractor on which the synchronized dynamics occur[14]. Its delimitation is important in order to characterize the global properties which influence the qualitative effects of riddling or blowout bifurcations. In fact, a minimal invariant absorbing area that surrounds a Milnor attractor defines a compact region of the phase plane that acts as a trapping bounded vessel inside which the trajectories starting near Δ are confined. This gives an upper bound for the oscillations (bursts) which characterize both the transient dynamics of the trajectories which eventually synchronize, and the persistent oscillations (on-off intermittency) which describe the dynamics just after a blowout bifurcation. Moreover, contacts between the portions of critical curves bounding the minimal absorbing area surrounding a Milnor attractor and the basin boundaries may mark the transition between local and global riddling phenomena, as it will be shown in the example below.

5.2 A competition model for market share

We consider a dynamic *brand competition model* proposed in Bischi et al., 2000a. This model describes a market where a population of consumers can choose between two brands of homogeneous goods, produced by two competing firms. Let x, y represent the marketing efforts of two firms (advertising, $R\&D$, etc.) and B the total sales potential of the market (in terms of customer market expenditures). Then the share of the market (sales revenue) accruing to firm 1 and to firm 2 is Bs_1 and $Bs_2 = B - Bs_1$, respectively, where

$$s_1 = \frac{ax^{\beta_1}}{ax^{\beta_1} + by^{\beta_2}} \ , \ s_2 = \frac{by^{\beta_2}}{ax^{\beta_1} + by^{\beta_2}} \quad . \tag{5.4}$$

The terms $A_1 = ax^{\beta_1}$ and $A_2 = by^{\beta_2}$ represent the recruitment of customers by firm 1 and 2, respectively, given x and y units of effort, and the parameters a and b denote the relative effectiveness of the effort made by the firms[15]. A dynamic model is obtained by assuming that the two competitors change their marketing efforts adaptively, in response

[14] Boundaries of trapping regions can also be obtained by the union of segments of critical curves and portions of unstable sets of saddle cycles, and in this case we have a so called *absorbing areas of mixed type* (see Mira et al., 1996). We don't enter here in such details, as in the example given below only standard absorbing areas (i.e. completely bounded by critical arcs) are present.

[15] Since $\frac{dA_1}{dx}\frac{x}{A_1} = \beta_1$ and $\frac{dA_2}{dy}\frac{y}{A_2} = \beta_2$, the parameters β_1 and β_2 denote the elasticities of the attraction of firm (or brand) i with regard to its effort.

to the profits achieved in the previous period:

$$T : \begin{cases} x(t+1) = x(t) + \lambda_1 x(t) \left(B \frac{x(t)^{\beta_1}}{x(t)^{\beta_1} + k y(t)^{\beta_2}} - x(t) \right) \\ y(t+1) = y(t) + \lambda_2 y(t) \left(B \frac{k y(t)^{\beta_2}}{x(t)^{\beta_1} + k y(t)^{\beta_2}} - y(t) \right) \end{cases} \tag{5.5}$$

where the parameters $\lambda_i > 0, i = 1, 2$, measure the rate of adjustment and $k = b/a$.

The map (5.5) is a noninvertible map of $Z_4 - Z_2 - Z_0$ type. The set of points for which $\det DT(x, y) = 0$ is given by the union of two branches, say $LC_{-1}^{(a)}$ and $LC_{-1}^{(b)}$, and the shape of the two branches of LC, $LC^{(a)} = T(LC_{-1}^{(a)})$ and $LC^{(b)} = T(LC_{-1}^{(b)})$, as well as the corresponding Riemann foliation, is similar to the one shown in Figure 9.

Following Kopel at al., 2000, Bischi and Gardini, 2000, let us consider the symmetric case of identical firms, obtained for $\lambda_1 = \lambda_2 = \lambda$, $\beta_1 = \beta_2 = \beta$ and $k = 1$, to show some applications of the methods described above. The restriction of the symmetric map to the invariant diagonal is given by

$$g(x) = (1 + \frac{1}{2}\lambda B)x - \lambda x^2. \tag{5.6}$$

which is conjugate to the standard logistic map (2.7), $z' = \mu z(1 - z)$, with $\mu = 1 + \frac{1}{2}\lambda B$, by the linear transformation $x = z\,(1 + \lambda B/2)\,/\lambda$. For the symmetric map, the Jacobian matrix, computed at a point of the diagonal Δ, is

$$DT(x, x; \lambda, B, \beta,) = \begin{bmatrix} 1 - 2\lambda x + \frac{\lambda B(\beta+2)}{4} & -\frac{\lambda B \beta}{4} \\ -\frac{\lambda B \beta}{4} & 1 - 2\lambda x + \frac{\lambda B(\beta+2)}{4} \end{bmatrix} . \tag{5.7}$$

Hence, the eigenvalues are $\lambda_{||} = 1 + \frac{1}{2}\lambda B - 2\lambda x$, $\lambda_\perp = 1 + \frac{1}{2}\lambda B(1 + \beta) - 2\lambda x$, and the transverse Lyapunov exponents are readily obtained:

$$\Lambda_\perp = \lim_{N \to \infty} \frac{1}{N} \sum_{n=0}^{N} \ln \left| 1 + \frac{1}{2}\lambda B(1 + \beta) - 2\lambda x_n \right| .$$

It is important to note that the parameter β only appears in the transverse eigenvalue $\lambda_\perp$, i.e. β is a *normal parameter*: It has no influence on the dynamics along the invariant submanifold Δ, and only influences the transverse stability. This allows us to consider fixed values of the parameters λ and B, such that a chaotic attractor $A_\Delta \subset \Delta$ of the map (5.6) exists, with an absolutely continuous invariant measure on it. So, we can study the transverse stability of A_Δ as the parameter β varies.

Suitable values of the aggregate parameter λB, at which chaotic intervals for the restriction (5.6) exist, are obtained from the well known properties of the logistic map (see e.g. Collet and Eckmann, 1980, Mira, 1987). For example, at the parameter value $\overline{\mu}_2 = 3.5748049387592...$ the period-4 cycle of the logistic map undergoes the homoclinic bifurcation, at which four cyclic chaotic intervals are obtained by the merging of 8 cyclic chaotic intervals. By using $\lambda B = 2(\overline{\mu}_2 - 1)$ we get a four-band chaotic set A_Δ along the diagonal Δ.

Figure 14 shows the results of the numerical computations of the natural transverse Lyapunov exponent $\Lambda_{\perp}^{nat}$ as β varies in the interval $(0, 0.2)$. Observe that a "window" of negative values of $\Lambda_{\perp}^{nat}$ is visible for $0.0575 < \beta < 0.1895$. For example, for $\beta = 0.09$ we have $\Lambda_{\perp}^{nat} = -8.36 \times 10^{-2} < 0$, and we expect that synchronization of the marketing efforts of the two firms occurs for a set of initial conditions with positive Lebesgue measure (this implies that trajectories that synchronize, even starting out of the diagonal, can be numerically observed). The issue of synchronization gets more complex in this case, however, because for this values of the parameters two coexisting attractors inside the feasible set can be numerically observed: the 4-cyclic chaotic set $A_{\Delta} \subset \Delta$ and an attracting cycle of period 2 with periodic points located out of Δ. In Figure 15 the coexisting attractors are represented by black points, each with its own basin of attraction: the white points represent the basin $\mathcal{B}(A_{\Delta})$ of the points generating trajectories that synchronize along A_{Δ}, whereas the light grey points represent the basin $\mathcal{B}(C_2)$ whose points generate trajectories converging to the stable cycle C_2. The dark-grey region represents the set of points which are not feasible, i.e., which generate trajectories involving negative values of the state variables.

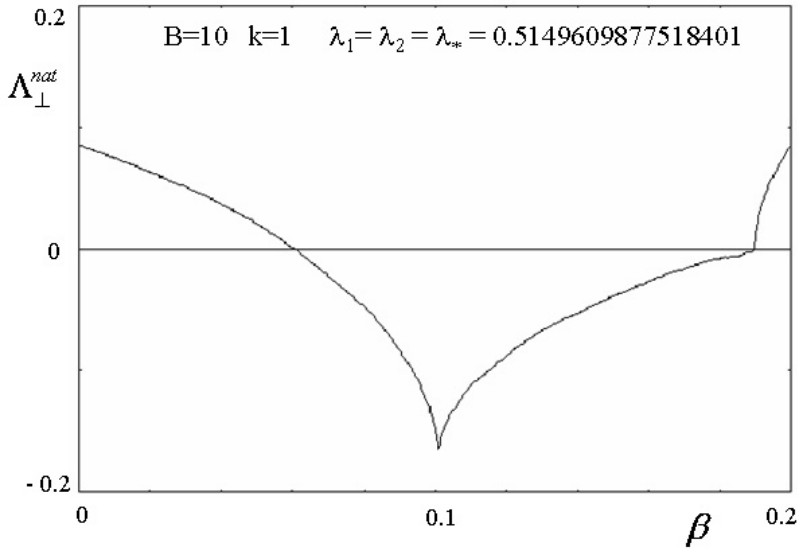

Figure 14.

For the set of parameters used in Figure 15, the four-band chaotic set A_{Δ}, embedded into the invariant diagonal Δ, is not a topological attractor however. In fact, an 8-cycle C_8 embedded inside the diagonal exists, which is transversely repelling. This means that trajectories starting along the local unstable set $W_{\perp}^{u}(C_8)$, issuing from the periodic points of C_8, as well as those starting from narrow tongues along $W_{\perp}^{u}(C_8)$ and from all

the infinitely many preimages of the periodic points of C_8 (such preimages are densely distributed along A_Δ due to the fact that A_Δ is a chaotic set with absolutely continuous invariant measure) are repelled away from the diagonal. So, if we consider a sufficiently small neighborhood W of A_Δ, we have that the local unstable set of the transversely unstable cycle intersects ∂W and a set of points with positive Lebesgue measure exists in W whose trajectories exit W in a finite number of iterations. This implies that no neighborhood $V \subset W$ exists such that the definition of Lyapunov stability holds. In this case it is possible to prove that, around the local transverse unstable set of a transversely unstable cycle, open sets of points exist, called "tongues" in Lai et al., 1996 or "wedges" in Alexander et al., 1992, such that the trajectories starting from points of these "tongues" exit W after a finite number of iterations. Similar "tongues" also exist in correspondence of the infinite preimages, along Δ, of the points of C_8. So, A_Δ is not a topological attractor for T, however it is an attractor in Milnor sense because $\Lambda_\perp^{nat} < 0$. In other words, most initial conditions close to A_Δ are attracted to A_Δ, but in any neighborhood of A there exists a dense set that is locally repelled in a direction transverse to it. As argued in the previous section, the locally repelled trajectories may eventually return to A_Δ (i.e. synchronize) after a transient phase in which they make several excursions (bursts) away of Δ, or they may belong to the basin $\mathcal{B}(C_2)$. In the latter case the basin of A_Δ is *riddled* with the basin of C_2. In our case, the locally repelled trajectories are folded back by the action of the global dynamical properties of the map T, and after a transient with some bursts away from Δ occurring, they synchronize in the long-run. The time evolution of the difference of the marketing efforts, $(x_t - y_t)$, during the transient portion of a typical trajectory, starting from the initial allocations $(x_0, y_0) = (6, 6.01)$, is shown in Figure 15b, where the early 300 iterates are represented. After about 40 periods the evolution of the system seems to have reached almost complete synchronization. During the next 40 periods the two competitors behave practically in the same way. At this point the trajectory seems to have definitively settled down on the attractor A_Δ (this would be the case for a topological attractor), and we would tend to conclude that the two-players model can be replaced by a one-player model. However, the trajectory then moves again far away from the diagonal, and the two competitors now act again in a very different fashion. Several bursts of the trajectory, out of Δ, are observed until perfect synchronization of the marketing efforts is eventually obtained. Such an intermittent behavior is a typical characteristic of the convergence to a non-topological Milnor attractor. The pattern of the time series resembles that of a system which is subject to exogenous random shocks, even if the dynamical system that generates such a pattern is completely deterministic. This peculiar dynamical behavior is related to the fact that even if the Milnor attractor attracts "on average" according to the fact that $\Lambda_\perp^{nat} < 0$, the presence of some transversely repelling cycles (even if less influent than the transversely attracting ones) causes sudden bursts when the trajectories happen to get close to them.

However, the locally repelled trajectories cannot reach the other attractor C_2. This is due to the presence of an absorbing area $\mathcal{A}$ around A_Δ, from which the trajectory starting close to A_Δ cannot escape. The boundary $\partial\mathcal{A}$ of such absorbing area, shown in Figure 16a, has been obtained following the procedure outline in the previous section:

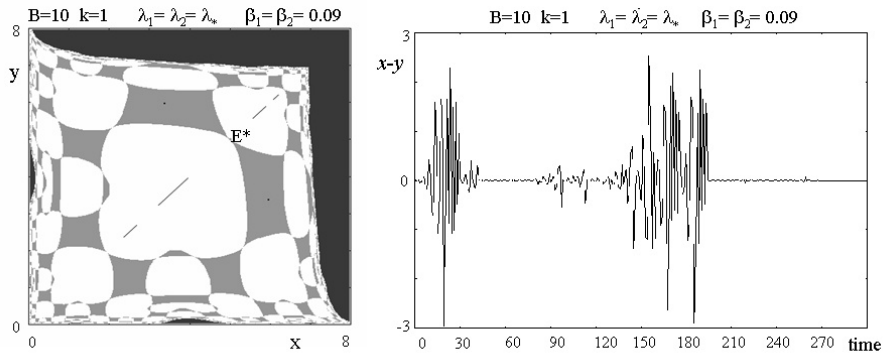

Figure 15.

starting from a portion of LC_{-1}, approximately taken in the region occupied by the area of interest, its images by T of increasing rank are computed until a closed region is obtained. In order to obtain the boundary of the absorbing area $\mathcal{A}$, six images of the generating arc γ are sufficient. However, only the portion of γ belonging to the branch $LC_{-1}^{(b)}$ has been used because the images of the other portion, the one belonging to the upper branch $LC_{-1}^{(a)}$, are always inside the absorbing area, so that they do not form part of the boundary. Hence in Figure 16a we have $\gamma = \mathcal{A} \cap LC_{-1}^{(b)}$ and $\partial\mathcal{A} \subset \bigcup_{k=1}^{6} T^k(\gamma)$.

We remark that $\mathcal{A}$ includes the Milnor chaotic attractor $A_\Delta \subset \Delta$, and all the trajectories starting from a neighborhood of A_Δ, cannot escape $\mathcal{A}$. Loosely speaking $\partial\mathcal{A}$ behaves as a bounded vessel for the intermittency phenomena related to the presence of the transversely repelling cycles embedded inside A_Δ. The local unstable sets of these cycles are folded back (reinjected) by the folding action of the critical curves that form $\partial\mathcal{A}$. The size of the absorbing area containing the Milnor attractor A_Δ gives us firstly an idea of the maximal difference between the marketing efforts of the two firms. Secondly, there is an inverse relationship between the longevity of transients and the values of the natural Lyapunov exponent $\Lambda_\perp^{nat}$. For values of the degree of competition β for which $\Lambda_\perp^{nat}$ is strongly negative the transient phase where bursts occur before the trajectories of marketing efforts settle down along the diagonal is relatively short. Neglecting this relatively short transient period we can conclude that the model of the representative player is a good approximation. On the other hand, if $\Lambda_\perp^{nat}$ is close to zero but negative, then the transient phase is rather long. Frequent and persistent bursts occur before the marketing efforts of the competitors synchronize. It might seem that this justifies, at least in the long run, the assumption, often made in economic models, that homogeneous agents can be considered as synchronized, so that their common behavior can be summarized by the behavior of a representative agent. However, in the situation shown in Figure 16a, the boundary of the absorbing area $\mathcal{A}$ is quite close to the boundary of the basin of the stable cycle C_2. Indeed, a small increase of β causes a contact between the absorbing area and the basin of C_2 which leads to the destruction of the absorbing

area, so that some of the trajectories that are repelled from A_Δ can converge to C_2, and the basin of A_Δ becomes riddled (Figure 16b). This example shows a transition from a locally riddled to a globally riddled dynamics caused by a contact between the boundary of a minimal invariant absorbing area and the boundary of its basin of attraction.

After this bifurcation, it is very difficult to forecast if two homogeneous agents will synchronize in the long run, because even starting from an initial condition very close to the diagonal Δ, i.e. such identical agents with quasi-identical starting efforts, the structure of the basins is such that any forecasting about synchronization has no practical meaning. So, the concept of representative agent cannot be applied in such a situation.

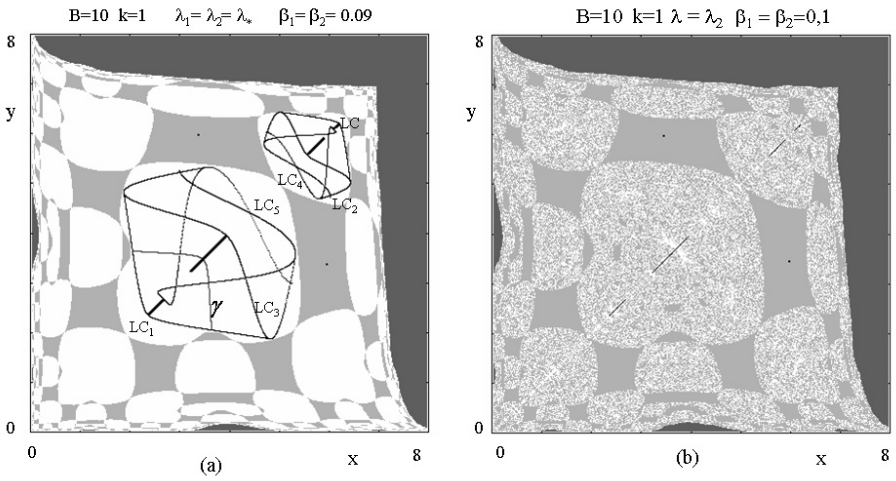

Figure 16.

5.3 Synchronization and partial synchronization in higher dimensional models

Some of the results stated above can be extended with more than two competitors. For example, let us consider a model that describes the interaction between three competitors, and assume that the time evolution of the system is described by the iteration of a map $T : (q_1(t), q_2(t), q_3(t)) \to (q_1(t+1), q_2(t+1), q_3(t+1))$ given by

$$T : \begin{cases} q_1' = T_1(q_1, q_2, q_3) \\ q_2' = T_2(q_1, q_2, q_3) \\ q_3' = T_3(q_1, q_2, q_3) \end{cases}$$

If all competitors are identical, then T is symmetric under the group of permutations

$$D_3 = \{M_{123}, M_{132}, M_{321}, M_{213}, M_{312}, M_{231}\}$$

where

$$M_{ijk}\begin{bmatrix} q_1 \\ q_2 \\ q_3 \end{bmatrix} = \begin{bmatrix} q_i \\ q_j \\ q_k \end{bmatrix} .$$

Obviously $M_{123} = I$ is the identity (trivial symmetry), whereas the three permutations of two coordinates

$$\begin{aligned} P_1(q_1, q_2, q_3) &= (q_1, q_3, q_2) \\ P_2(q_1, q_2, q_3) &= (q_3, q_2, q_1) \\ P_3(q_1, q_2, q_3) &= (q_2, q_1, q_3) \end{aligned}$$

represent reflections through the planes

$$\begin{aligned} \Pi_1 &= \{(q_1, q_2, q_3) \mid q_2 = q_3\}; \\ \Pi_2 &= \{(q_1, q_2, q_3) \mid q_1 = q_3\}; \\ \Pi_3 &= \{(q_1, q_2, q_3) \mid q_1 = q_2\} \end{aligned}$$

and the two cyclic permutations of the three coordinates

$$R_3^1 : (q_1, q_2, q_3) \to (q_3, q_1, q_2) \text{ and } R_3^2 : (q_1, q_2, q_3) \to (q_2, q_3, q_1)$$

represent rotations of $\frac{2}{3}\pi$ around the diagonal $S = \{q_1 = q_2 = q_3\}$.
A dynamical system with a symmetry M has a linear invariant subspace, given by the set of fixed points of M. In particular, Π_i are invariant two-dimensional submanifold for T, and the trajectories embedded inside Π_i, governed by the two-dimensional restriction of T to Π_i are called *partially synchronized* (two of the three players move in a synchronized way). Moreover, the intersection of the three invariant planes Π_i, given by $S = \left\{(q, q, q) \in \mathbb{R}^3\right\}$ is an invariant one-dimensional submanifold, and the trajectories embedded inside S, governed by the one-dimensional restriction of T to S, are *fully synchronized trajectories*. More generally, with n identical competitors, we can have *clusters* of $k \leq n$ synchronized competitors coexisting with non-synchronized ones.

Bibliography

R. Abraham, L. Gardini and C. Mira. *Chaos in discrete dynamical systems (a visual introduction in two dimension)*. Springer-Verlag, 1997.

H.N. Agiza, G.I. Bischi, and M. Kopel. Multistability in a Dynamic Cournot Game with Three Oligopolists. *Mathematics and Computers in Simulation*, **51**, 63-90, 1999.

A. Agliari, G.I. Bischi, and L. Gardini. Some methods for thr Global Analysis of Dynamic Games represented by Noninvertible Maps. In T. Puu and I. Sushko, editors, *Oligopoly Dynamics: Models and Tools*, Springer Verlag, pp. 31-83, 2002.

J.C. Alexander, J.A. Yorke, Z. You, and I. Kan. Riddled basins. *Int. Jou. of Bif. & Chaos*, **2**, 795-813, 1992.

M. Aoki, *New Approaches to Macroeconomic Modelling*. Cambridge University Press, New York, 1996.

P. Ashwin, J. Buescu, and I. Stewart. From attractor to chaotic saddle: a tale of transverse instability. *Nonlinearity*, **9**, 703-737, 1996.

E. Barucci, G.I. Bischi, and L. Gardini. Endogenous fluctuations in a bounded rationality economy: learning non perfect foresight equilibria. *Journal of Economic Theory*, 87, 243-253, 1999.

K. Binmore. *Fun and Games*. D.C. Heath, 1992.

G.I. Bischi, R. Carini, L. Gardini, and P. Tenti. *Sulle Orme del Caos. Comportamenti complessi in modelli matematici semplici*. Bruno Mondadori Editore, 2004.

G.I. Bischi, H. Dawid, and M. Kopel. Gaining the Competitive Edge Using Internal and External Spillovers: A Dynamic Analysis. *Journal of Economic Dynamics and Control*, vol. 27, 2171-2193, 2003a.

G.I. Bischi, H. Dawid, and M. Kopel. Spillover Effects and the Evolution of Firm Clusters. *Journal of Economic Behavior and Organization*, vol. 50, 47-75, 2003b.

G.I. Bischi, M. Gallegati, and A. Naimzada. Symmetry-Breaking bifurcations and representative firm in dynamic duopoly games. *Annals of Operations Research*, **89**, 253-272, 1999a.

G.I. Bischi and L. Gardini. Role of invariant and minimal absorbing areas in chaos synchronization. *Physical Review E*, **58**, 5710-5719, 1998.

G.I. Bischi and L. Gardini. Global Properties of Symmetric Competition Models with Riddling and Blowout Phenomena. *Discrete Dynamics in Nature and Society*, vol. 5, 149-160, 2000.

G.I. Bischi, L. Gardini, and M. Kopel. Analysis of Global Bifurcations in a Market Share Attraction Model. *Journal of Economic Dynamics and Control*, **24**, 855-879, 2000a.

G.I. Bischi, L. Gardini, and C. Mira. Plane maps with denominator. Part I: some generic properties. *International Journal of Bifurcation and Chaos,* **9(1)**, 119-153, 1999b.

G.I. Bischi, L. Gardini, and C. Mira. Plane Maps with Denominator. Part II: Noninvertible maps with simple focal points. *International Journal of Bifurcation and Chaos*, vol. 13, No. 8, 2253-2277, 2003c.

G.I. Bischi and M. Kopel. Equilibrium Selection in a Nonlinear Duopoly Game with Adaptive Expectations. *Journal of Economic Behavior and Organization*, **46(1)**, 73-100, 2001.

G.I. Bischi and F. Lamantia. Nonlinear Duopoly Games with Positive Cost Externalities due to Spillover Effects. *Chaos, Solitons & Fractals*, vol. 13, 805-822, 2002a.

G.I. Bischi and F. Lamantia. Chaos Synchronization and Intermittency in a Duopoly Game with Spillover Effects. Chapter 8 in T. Puu and I. Sushko, editors, *Oligopoly Dynamics: Models and Tools*, Springer Verlag, 195-217, 2002b.

G.I. Bischi, C. Mammana, and L. Gardini. Multistability and cyclic attractors in duopoly games. *Chaos, Solitons & Fractals*, **11**, 543-564, 2000b.

G.I. Bischi, L. Mroz, and H. Hauser. Studying basin bifurcations in nonlinear triopoly games by using 3D visualization. *Nonlinear Analysis, Theory, Methods & Applications,* **47(8)**, 5325-5341, 2001.

G.I. Bischi and A. Naimzada. Global Analysis of a Duopoly game with Bounded Rationality. *Advances in Dynamic Games and applications*, vol.5, 361-385, Birkhauser, 2000.

W.A. Brock, C. Hommes. A Rational Route to Randomness. *Econometrica*, 65,1059-1095, 1997.

J. Buescu. *Exotic Attractors*, Birkhäuser, Boston, 1997.

C. Chiarella, R. Dieci, and L. Gardini. Asset price dynamics in a financial market with fundamentalists and chartists. *Discrete Dynamics in Nature and Society*, Vol 6, 69-99, 2001.

C. Chiarella, R. Dieci, and L. Gardini. Speculative Behaviour and Complex Asset Price Dynamics: A Global Analysis. *Journal of Economic Behavior and Organization*, 49(1) 173-192, 2002.

P. Collet and J.P. Eckmann. *Iterated maps on the interval as dynamical systems*, Birkhäuser, Boston, 1980.

R.L. Devaney. *An Introduction to Chaotic Dynamical Systems.* The Benjamin / Cummings Publishing Co., Menlo Park, California, 1987.

R. Dieci, G.I. Bischi, and L. Gardini. Multistability and role of noninvertibility in a discrete-time business cycle model. *CEJOR*, vol. 9, 71-96, 2001.

A. Ferretti and N.K. Rahman. A study of coupled logistic maps and its applications in chemical physics. *Chemical Physics*, 119, 275-288, 1988.

H. Fujisaka and T. Yamada. Stability theory of synchronized motion in coupled-oscillator systems. *Progress of Theoretical Physics*, **69 (1)**, 32-47, 1983.

C. Grebogi, E. Ott, and J.A. Yorke. Crises, sudden changes in chaotic attractors and transient chaos. *Physica* **7**D, 81-200, 1983.

J. Guckenheimer and T. Holmes. *Non-linear Oscillations, Dynamical Systems, and Bifurcations of Vector Fields.* Springer, 1983.

R. Guesnerie and M. Woodford. Endogeneous fluctuations. In J. Laffont, editor, *Advances in Economic Theory*, 288-412, Cambridge University Press, 1993.

I. Gumowski and C. Mira. *Dynamique Chaotique,* Cepadues Editions, Toulose, 1980.

M. Hasler and Y. Maistrenko. An introduction to the synchronization of chaotic systems: coupled skew tent maps. *IEEE Trans. Circuits Syst.*, **44 (10),** 856-866, 1997.

A. P. Kirman. Whom or What Does the Representative Individual Represent? *Jou. of Econ. Perspectives,* 6, 117-136, 1992.

M. Kopel. Simple and Complex Adjustment Dynamics in Cournot Duopoly Models. *Chaos, Solitons & Fractals*, **7(12)**, 2031-2048, 1996.

M. Kopel, G.I. Bischi, and L. Gardini. On new phenomena in dynamic promotional competition models with homogeneous and quasi-homo-geneous firms. In D. Delli Gatti, M. Gallegati, and A.P. Kirman, editors, *Interaction and Market Structure. Essays on Heterogeneity in Economics.* Springer-Verlag, pp. 57-87, 2000.

Y.C. Lai, C. Grebogi, and J.A. Yorke. Riddling bifurcation in chaotic dynamical systems. *Physical Review* Letters*,* 77, 55-58, 1996.

Y.C. Lai and C. Grebogi. Noise-induced riddling in chaotic systems. *Physical Review Letters* **77**, 5047-5050, 1996.

H.W. Lorenz. Multiple attractors, Complex Basin Boundaries, and Transient Motion in Deterministic Economic Systems. In G. Feichtinger, editor, *Dynamic Economic Models and Optimal Control*, 411-430, North-Holland, Amsterdam, 1992.

Y. Maistrenko, T. Kapitaniak, and P. Szuminski. Locally and globally riddled basins in two coupled piecewise-linear maps. *Physical Review E*, **57 (3)**, 6393-6399, 1997.

Y. Maistrenko, V.L. Maistrenko, A. Popovich, and E. Mosekilde. Role of the Absorbing Area in Chaotic Synchronization. *Physical Review Letters*, **80 (8)**, 1638-1641, 1998a.

Y. Maistrenko, V.L. Maistrenko, A. Popovich, and E. Mosekilde. Transverse instability and riddled basins in a system of two coupled logistic maps. *Physical Review E*, **57 (3)**, 2713-2724, 1998b.

J. Milnor. On the concept of attractor. *Commun. Math Phys*, **99**, 177-195, 1985.

C. Mira. *Chaotic Dynamics*. Word Scientific, Singapore, 1987.

C. Mira, J.P. Carcasses, G. Millerioux, and L. Gardini. Plane foliation of two-dimensional noninvertible maps. *International Journal of Bifurcation & Chaos*, vol.6 (8), 1439-1462, 1996.

C. Mira, D. Fournier-Prunaret, L. Gardini, H. Kawakami, and J.C. Cathala. Basin bifurcations of two-dimensional noninvertible maps: fractalization of basins. *International Journal of Bifurcation and Chaos*, **4**, 343-381, 1994.

C. Mira, L. Gardini, A. Barugola, and J.C. Cathala. *Chaotic Dynamics in Two-Dimensional Noninvertible Maps*, World Scientific, Singapore, 1996.

C. Mira and C. Rauzy. Fractal aggregation of basin islands in two-dimensional quadratic noninvertible maps. *International Journal of Bifurcations and Chaos*, **5(4)**, 991-1019, 1995.

Y. Nagai and Y.C. Lai. Periodic-orbit theory of the blowout bifurcation. *Physical Review E*, **56 (4)**, 4031-4041, 1997.

E. Ott and J.C. Sommerer. Blowout bifurcations: the occurrence of riddled basins and on-off intermittency. *Phys. Lett. A*, **188**, 39-47, 1994.

L.M. Pecora and T.L. Carrol. Synchronization in chaotic systems. *Physical Review Letters*, **64 (8)** pp. 821-824, 1990.

T. Puu. *Attractors, Bifurcations and Chaos*. Springer Verlag, Berlin, 2000.

A.S. Soliman. An analysis of the effectiveness of policy based on basins of attraction. *Journal of Macroeconomics*, 21, 165-178, 1999.

S.C. Venkataramani, B.R. Hunt, and E. Ott. Bubbling transition. *Physical Review E*, **54**, 1346-1360, 1996.

J.W. Weibull, *Evolutionary Game Theory*. The MIT Press, 1995.